

STUDY OF THE POSSIBILITY OF THE DETECTION OF FLUORESCENT DYES
BY CATHODOLUMINESCENCE IN THE SCANNING ELECTRON MICROSCOPE

and

PARTIAL DENATURATION MAPS OF LAMBDA DNA
USING METHYLMERCURIC HYDROXIDE

Thesis by

Douglas Crane Mohr

In Partial Fulfillment of the Requirements
for the Degree of
Doctor of Philosophy

California Institute of Technology
Pasadena, California

1973

(Submitted November 20, 1972)

Acknowledgments

I would like to acknowledge all of the people who have helped me during my stay at Cal Tech. Especially, I would like to thank Chong Sung Lee, Ray Bowman, and Carl Schmid for many valuable discussions.

The work at J.P.L. would not have been possible without the assistance of many people. Bob Frazer, Tom Andrews, and Elbert Johnson were particularly helpful during the assembly and testing of the scanning electron microscope.

For financial support, I would like to thank my parents, the National Institutes of Health for U.S.P.H.S. Grants Nos. GM 01262 and GM 10991, and the California Institute of Technology President's Fund Grant PF-010.

Finally, I would like to acknowledge the assistance and guidance of Norman Davidson. His great capability as a teacher and a scientist sets an inspiring example.

Abstract

Part 1. The possibilities of using ethidium bromide, quinacrine hydrochloride, and dansyl chloride as cathodoluminescent stains for scanning electron microscopy have been investigated. Nucleic acid specimens stained with the dyes gave best results when they were embedded in frozen glycerol and examined at liquid nitrogen temperature. Under these conditions, the excitation cross section for ethidium bromide is about 0.5 A^2 and the destruction cross section 5 A^2 . The other dyes were destroyed quite rapidly.

Even under the best conditions, the minimum amount of ethidium bromide detectable by cathodoluminescence is about the same as detectable by fluorescence microscopy.

Part 2. Methylmercuric hydroxide preferentially reacts with thymine. This reaction disrupts the Watson-Crick base pairing, the mercurated regions appearing as loops in the electron microscope. Lambda DNA has been partially denatured by methylmercuric hydroxide and mounted for electron microscopy by the basic film technique.

The results indicate that there are four regions which readily denature, located on one side of the lambda genome. This result is in agreement with other thermal and alkaline partial denaturation data.

Table of Contents

	<u>Page</u>
Acknowledgments	ii
Abstract	iii
Part 1. Study of the Possibility of the Detection of Fluorescent Dyes by Cathodoluminescence in the Scanning Electron Microscope . . .	1
References	59
Part 2. Partial Denaturation Maps of Lambda DNA using Methylmercuric Hydroxide	63
References	85
Propositions	86

Part 1

STUDY OF THE POSSIBILITY OF THE DETECTION OF FLUORESCENT DYES
BY CATHODOLUMINESCENCE IN THE SCANNING ELECTRON MICROSCOPE

Introduction

In conventional transmission electron microscopy the contrast of the different structures in a biological specimen is usually developed by deposition of heavy metal stains such as MnO_2 (from KMnO_4), or Os (from OsO_4 staining). The chemistry of the processes responsible for the deposition of the metals is obscure and the reactions are usually nonspecific.

On the contrary, the chemistry of attaching fluorescent dyes to specific substances in biological specimens is much more precise (although this too isn't as specific as one might desire). There are fluorescent dyes which bind specifically to nucleic acids. There are other dyes which bind specifically to the active sites of enzymes. Fluorescent dyes can be coupled to reagents which themselves specifically react with functional groups of proteins. Given the incentive, one can anticipate further developments in this field, since it is one to which rational organic chemistry can be applied.

However, the localization of a fluorescent dye, by its light emission, has a resolution of the order of $\frac{1}{2}$ of the wavelength of the light and therefore only about 2000 Å at best. We propose an alternate method

for locating the fluorescent dyes in a specimen. The fluorescence will be excited by electron beam irradiation. The electron beam can be focused on an area of the specimen which is limited by the resolution of the electron optics and practically at present can be 100 Å x 100 Å. The emission of light will be detected by conventional photoelectric methods which are of high sensitivity but the resolution will be dependent on electron optics.

The scanning electron microscope (SEM) in which a focused beam of electrons scans a specimen in two dimensions is an ideal instrument for our purposes. In its conventional mode of operation, the quantity observed in the SEM is the number of secondary electrons emitted from each point in the sample.

The alternative mode of operation, in which the light excited by the scanning electron beam is detected, is called the cathodoluminescent (CL) mode. The idea of using CL to localize specific chemicals by scanning electron microscopy is not new (1, 2, 3). However, no one has seriously tried to use the state of the art staining technology and photon detection to critically test the idea. The objective of this research was a critical study of the potentialities of cathodoluminescence in scanning electron microscopy.

In the CL mode, we want to detect light emitted from a selectively bound dye and discriminate this from any non-dye emission using an electron beam for excitation. To quantitatively evaluate this system, we need to determine the magnitudes of : the background (non-dye) emission, the dye emission (σ_{ex}), and the beam induced dye destruction (σ_d). In order to obtain these values we need a scanning electron microscope calibrated to measure the actual number of photons as a function of wavelength for background and dye specimens, and the beam current. The SEM must also be capable of providing an electron dose high enough to destroy part of the dye so that σ_d , the destruction cross section, can be evaluated.

Before the SEM was completed, some preliminary experiments were performed using a conventional transmission electron microscope as an electron source. Although the instrument was not photometrically calibrated nor capable of irradiating specimens with high doses of electrons (number of electrons per unit area), several things were learned. First, any transparent material such as glass, silica, polyethylene, polystyrene, or frozen glycerol emit a bluish light under electron bombardment (4, 5). Second, all of the fluorescent dyes tested, ethidium bromide (EB), acridine orange, coriphosphine O, and thioflavin T, emitted more

fluorescence while at liquid nitrogen temperatures in a frozen glycerol glass than at room temperature. Third, ethidium bromide, which is known to bind selectively to nucleic acids (6), was not destroyed by the beam as were the others.

Ethidium bromide seemed to have the best qualities for CL work of all the dyes tested. In addition, its fluorescence is in the red (6). Therefore, by using optical filters, EB fluorescence can be distinguished from the bluish background emission. For these reasons, most SEM experiments were designed to compare excitation and destruction cross sections of ethidium bromide bound to DNA under varying conditions. In this manner, the effects of temperature, and various embedding materials could be studied. Once favorable conditions were found, cross sections for dansyl chloride and quinacrine HCl were also obtained. These dyes were chosen in particular because of their importance to biology, dansyl for labelling proteins, and quinacrine for chromosome karyotyping.

The results indicate that none of the dyes tested emitted light as well as a regular phosphor under electron bombardment. At best, under practical operating conditions (the dyes were embedded in frozen glycerol) one or two photons are emitted per incident electron

with the dyes whereas a phosphor emits hundreds of photons. The dye dansyl chloride was destroyed by the beam very rapidly. The other dyes were destroyed at a rate 10 to 20 times greater than the rate of light emission. In other words, extensive electron bombardment of 10 or 20 dye molecules results in the production of one photon. At room temperature, with no glycerol, the situation is worse; 600 dye molecules are destroyed before a photon is produced.

Experimental

The Scanning Electron Microscope. It was desired to obtain the cross sections for excitation and destruction for a dye using an electron beam for excitation. To calculate these cross sections it is necessary to irradiate a known concentration of dye with a known number of electrons per unit area and to measure the number of photons emitted. An SEM equipped with a calibrated light measuring and current measuring devices is therefore necessary. In addition, it was desired to cool the specimen to liquid nitrogen temperatures. An instrument that could be adapted to these experiments was available at the Jet Propulsion Laboratories (JPL).

The microscope was designed and built at JPL by

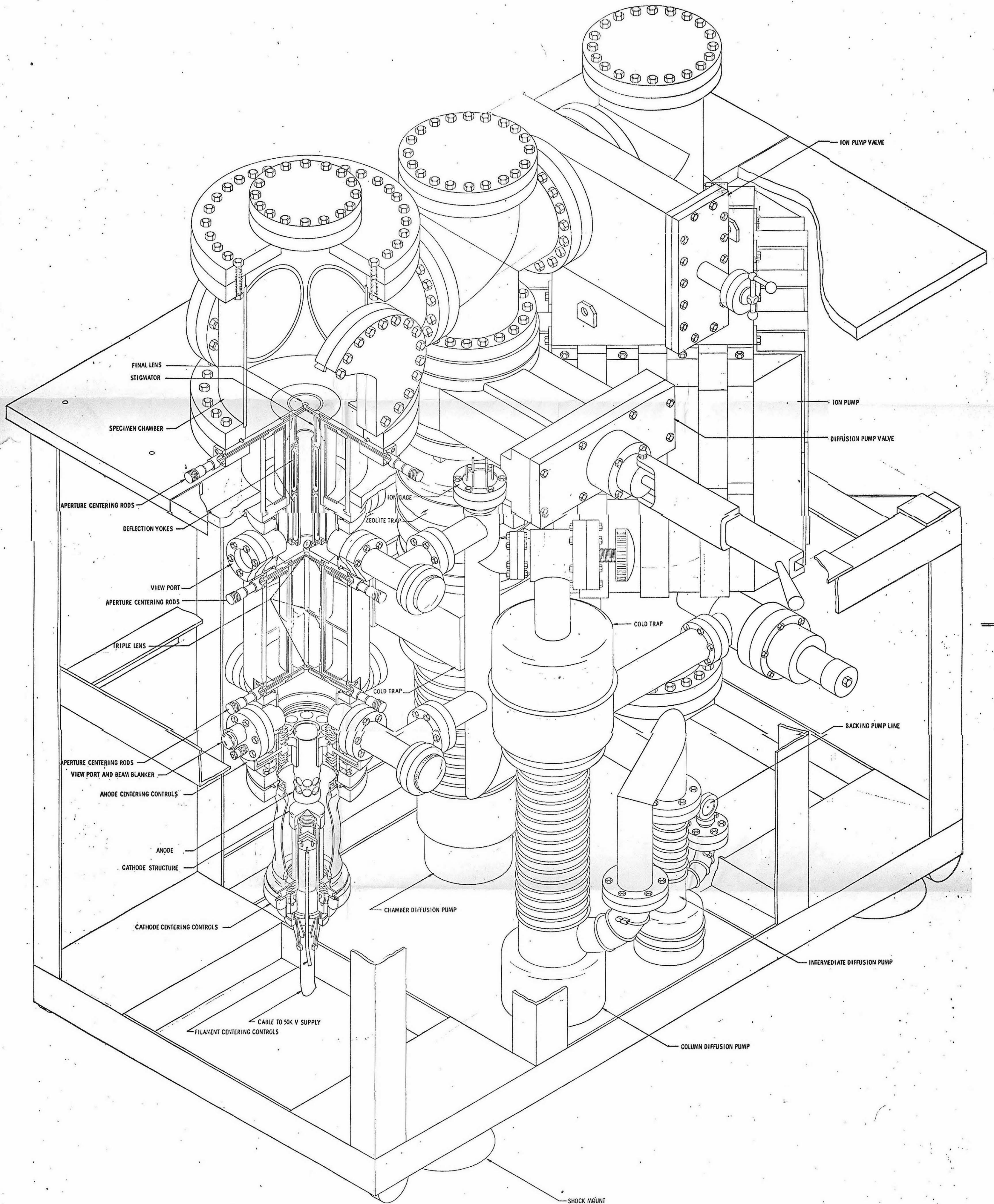
Mr. R. Frazer and T. Andrews. Figure 1 shows a diagram of the instrument without the stage or light measuring equipment. The microscope has a conventional hairpin filament and 4 electromagnetic lenses. Theoretically, it was designed to produce a 50 Å diameter electron beam although this goal was never achieved.

Electron Optics. The electron source is a conventional hairpin filament, self biased triode gun. This source produced a 100 micron sized virtual image which is demagnified further by the lenses. The filament and cathode structure surrounding it are at a high negative potential. The anode and the rest of the instrument are at ground potential.

The electrons travel through the anode and up the column into the triple lens. This multiple lens was designed with three gaps, spaced at 10 cm intervals and one winding, powering all three lenses. Each lens was designed to operate at a focal length of 1 cm. Most of the demagnification needed to get a 50 Å spot was intended to take place in this lens. Unfortunately, the triple lens has never operated properly. Aberrations within this lens prevent using it at all! No conditions of lens excitation could be found that would reduce the spot size. Reluctantly, the lens was abandoned.

The electrons next enter the scan deflection

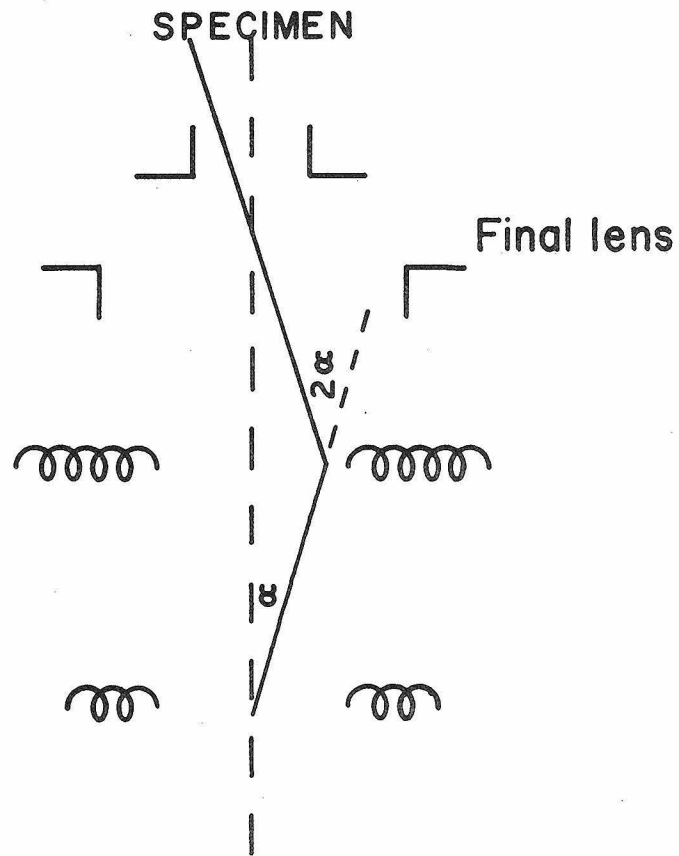
Figure 1. Line drawing of the scanning electron microscope. The scale is about $1/4$ of the actual size.



yokes. Here the electrons are deflected twice, first by an angle α and then eight cm up the column, by an angle 2α . Figure 2 shows the relationship of the deflection yokes and the final lens. No matter how much the beam is deflected, it will always toggle through the same point, the center of the final lens. In actual practice, electrons from the gun are focussed by the final lens only onto the specimen. Geometrically, the expected spot size from this operating configuration is 2 microns, which was found to be the case. A resolution of 2 microns for an instrument of this type is very poor, but no way has been found to improve it. All experiments were conducted with the instrument operating in this manner. Other than spray apertures, one 250 micron aperture was used in the final lens.

It is fortunately not necessary to have a 50 A diameter electron spot to obtain the data needed to calculate the cross sections. The 2 micron diameter beam was small enough and intense enough for that purpose.

Very recently it was found that pushing the two pole pieces of the triple lens to the bottom, creating a single lens, gave better results. A spot size of 2000 A was obtained on the first trial with this configuration.



Deflection Yokes

FIG 2

Figure 2. Schematic of the scan deflection system. Designed so that the beam toggles through the center of the final lens.

The Scan Generator. The scan generator provides the signal that moves the beam in a raster. In normal operation, the X and Y axis signal from the scan generator drives the X and Y deflection yoke amplifiers and the X and Y axes of a display cathode ray tube (CRT). The Z or intensity axis of the display CRT is modulated by the output of a detector to produce an image. The X and Y axis signals to the deflection amplifiers can be attenuated to adjust the magnification.

The scan generator output is digital and divides each axis into 1024 points (or pixels as they are termed). Thus each scan has a maximum of $(1024)^2$ or about 10^6 pixels. The starting and stopping pixels as well as the time per pixel can be selected.

Most experiments were performed with the scan parameters set as follows: $n \leq x \leq n+50$; $0 \leq y \leq 1024$, time per pixel = 512×10^{-6} sec. The time for such a scan would be $(n+50 - n)(1024)(512 \times 10^{-6} \text{ sec})$ which is about 25 seconds. The scan (x, y) would progress (n, 0), (n+1, 0), ..., (n+50, 0), (n, 1), ..., ..., (n+50, 1024). The scan generator Y axis signal was usually plotted against the Z axis signal (the CL detector output) on the X and Y axes of an oscilloscope. The detector output was noisy due to the simultaneous rapid X scanning as well as shot noise etc.; so the

signal was passed through a 10 Hz cut off filter before being displayed on the vertical (Y) axis of the oscilloscope. A block diagram of the electronics is given in figure 3.

Vacuum System. The original design of the microscope included diffusion as well as an ion pump so that a field emission electron source could be used. However, it was found that the magnetic field from the ion pump, passing freely through the stainless steel column, deflected the beam so badly that the instrument couldn't be aligned. Plate 1 shows the ion pump with the magnets removed; it was never used. Vacuums of 10^{-4} to 10^{-5} torr were routinely obtained in the microscope by means of diffusion pumps. A four inch diffusion pump was connected to the column (see Plate 2) and a six inch diffusion pump to the sample chamber. One mechanical pump and a two inch diffusion pump (see Plate 1) backed the two large diffusion pumps. Another mechanical pump was used when needed to rough pump the system down to a pressure of 100 microns.

The diffusion pumps used a total of 16 amps at 117 v AC. This produced an alternating magnetic field which caused the beam to oscillate at 60 Hz, degrading the resolution. A large three phase, full wave rectifier

Figure 3. Block outline of the electronics used to measure the excitation and destruction cross sections.

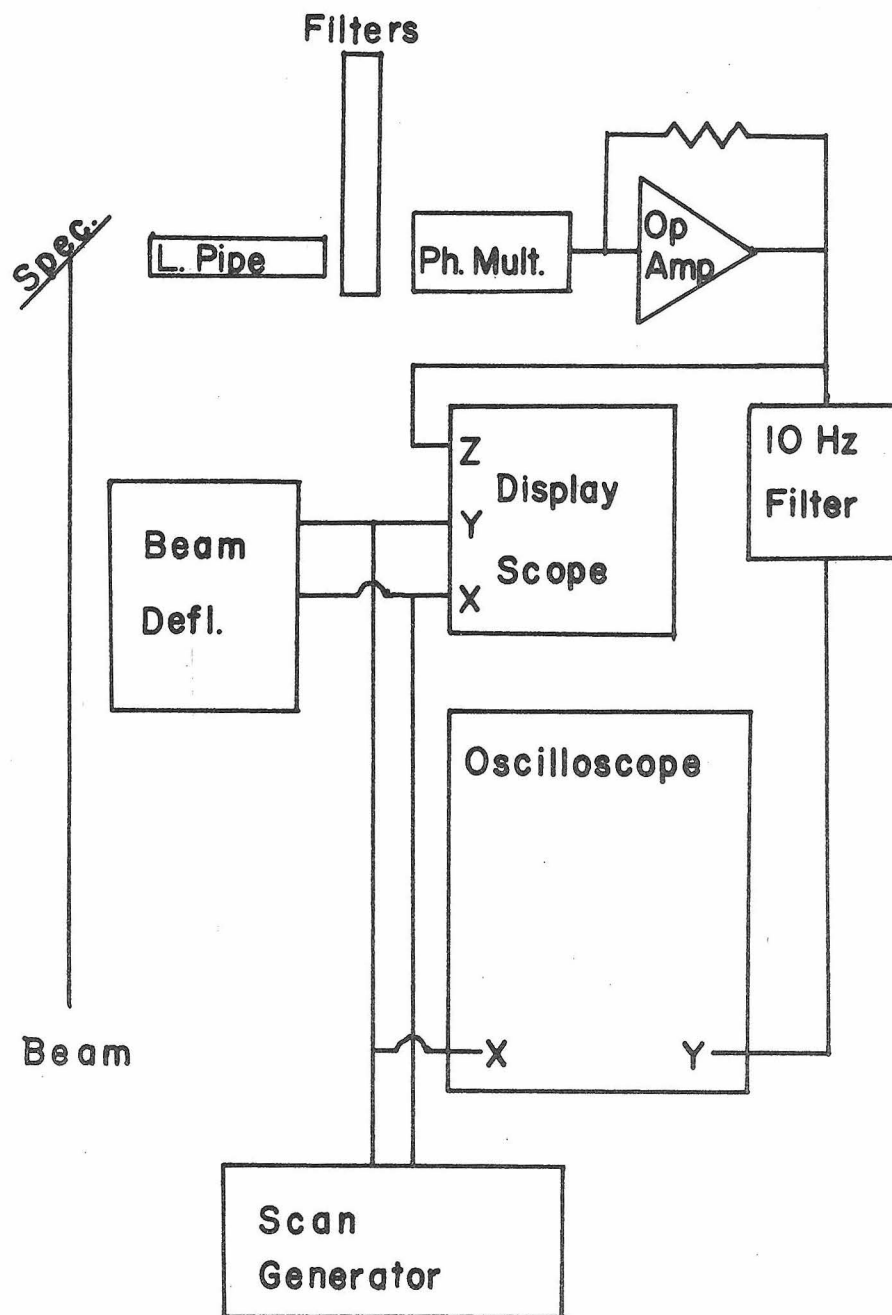
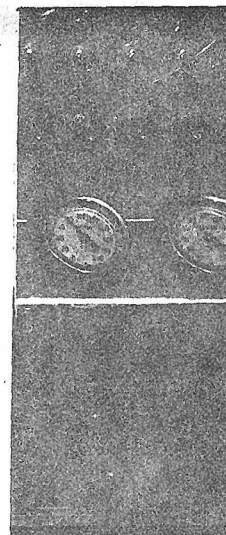
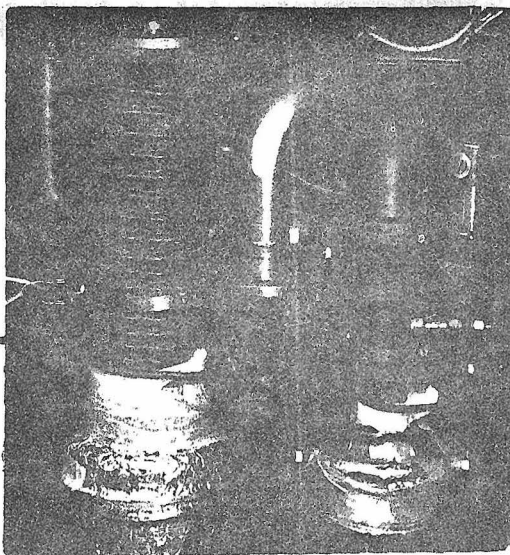
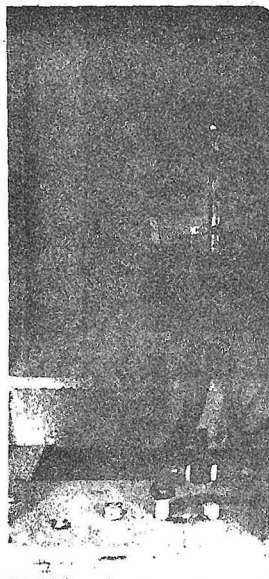
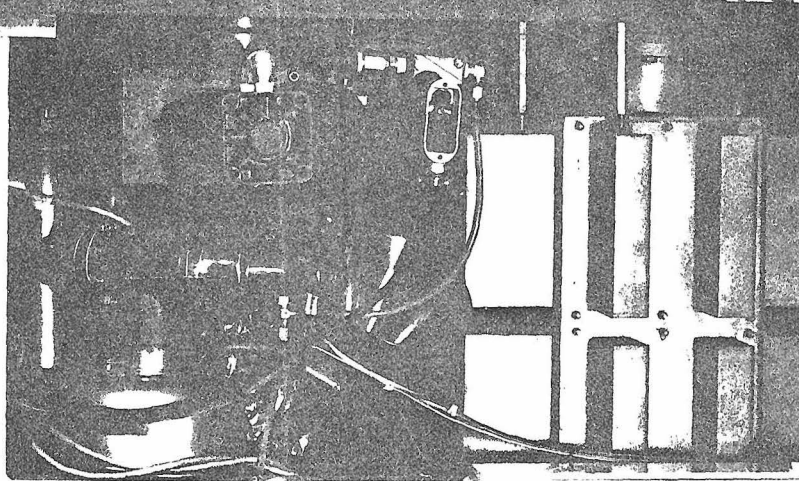
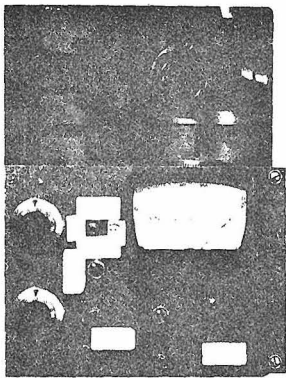
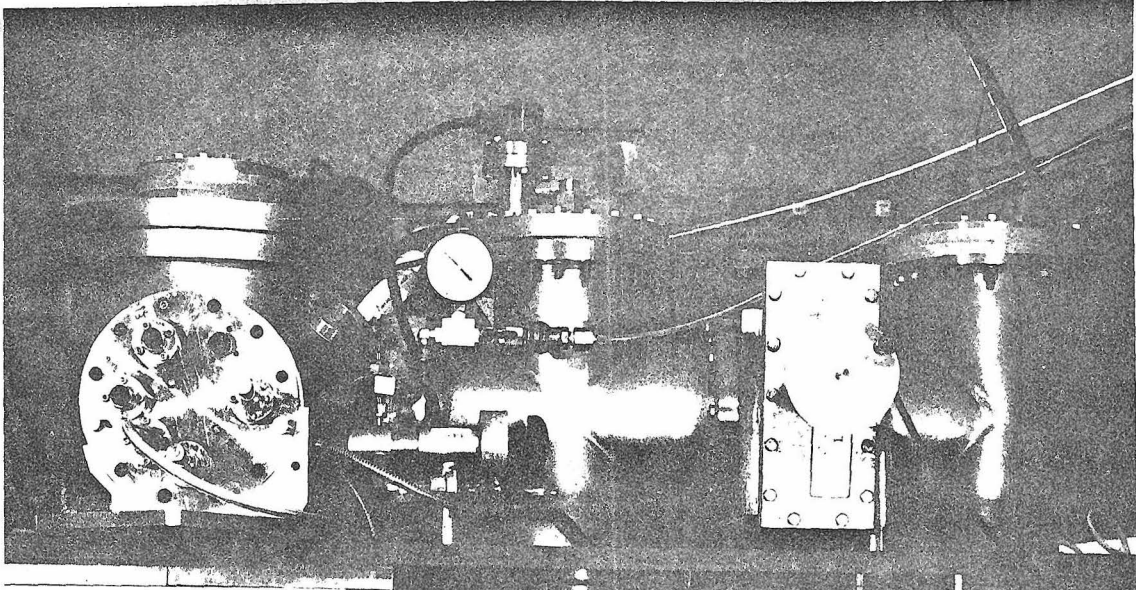
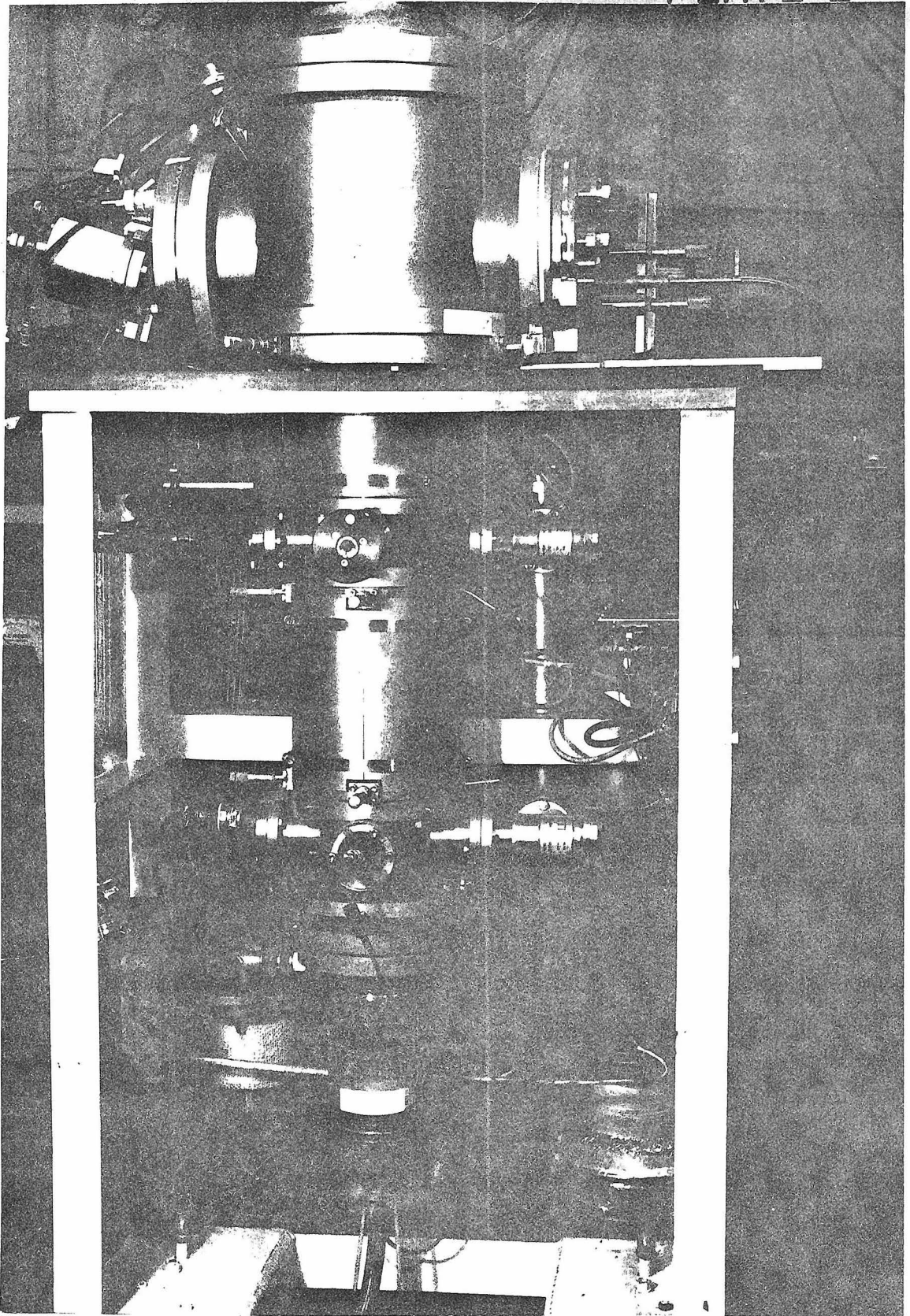


FIG 3

Plate 1. A side view of the scanning electron microscope. The column is on the left side, and the ion pump without magnets on the right.

Plate 2. A front view of the scanning electron microscope showing the column and electron gun (bottom).





was finally constructed so that the diffusion pumps could be run on direct current. It was also necessary to move the mechanical pumps some distance away from the column because of the alternating magnetic field problem.

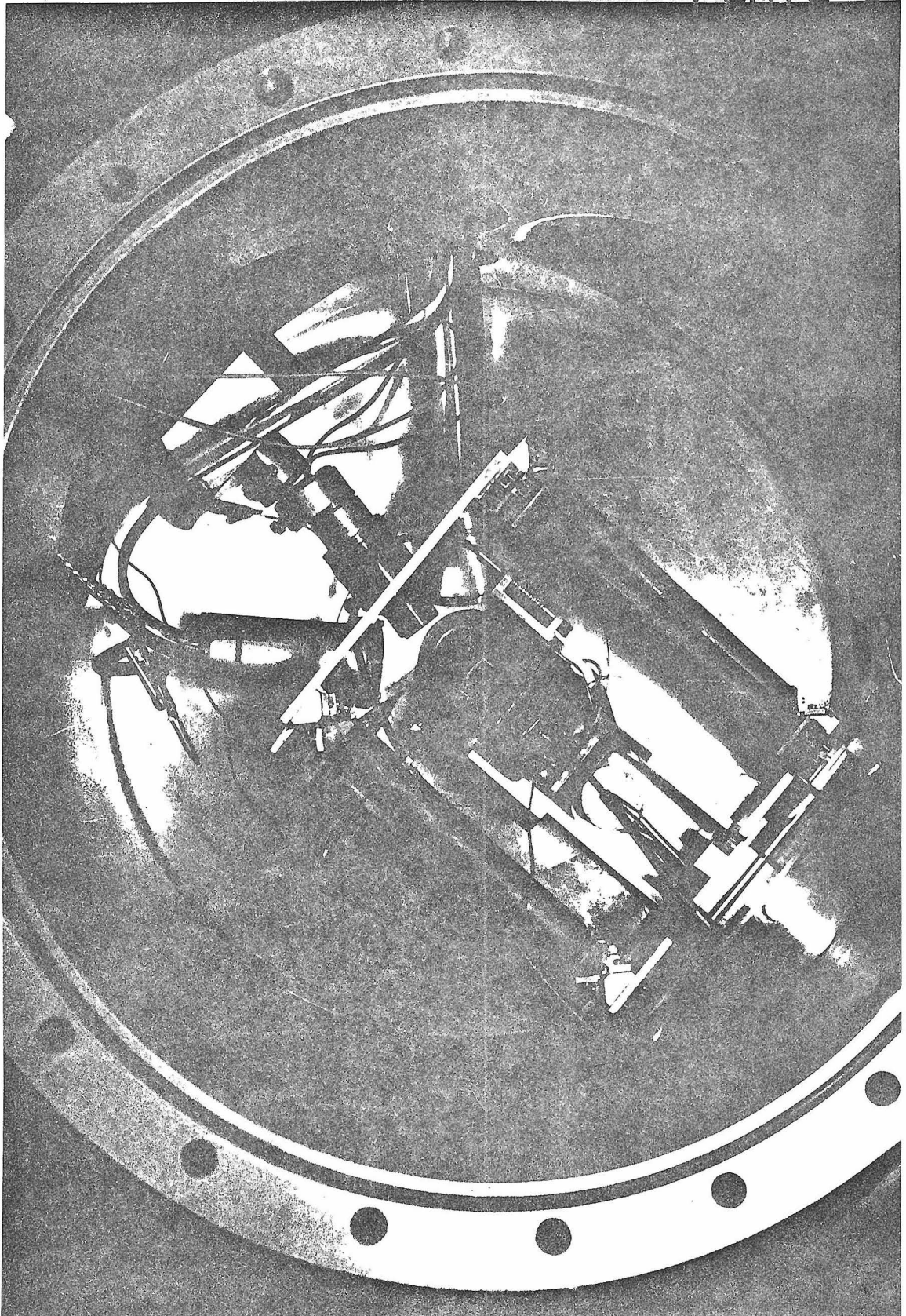
All of the diffusion pumps used polyphenyl ether as the working fluid. Vapors from this material decomposed in the beam to deposit a fluorescent contaminant. This was eliminated by using liquid nitrogen traps between the microscope and the pumps.

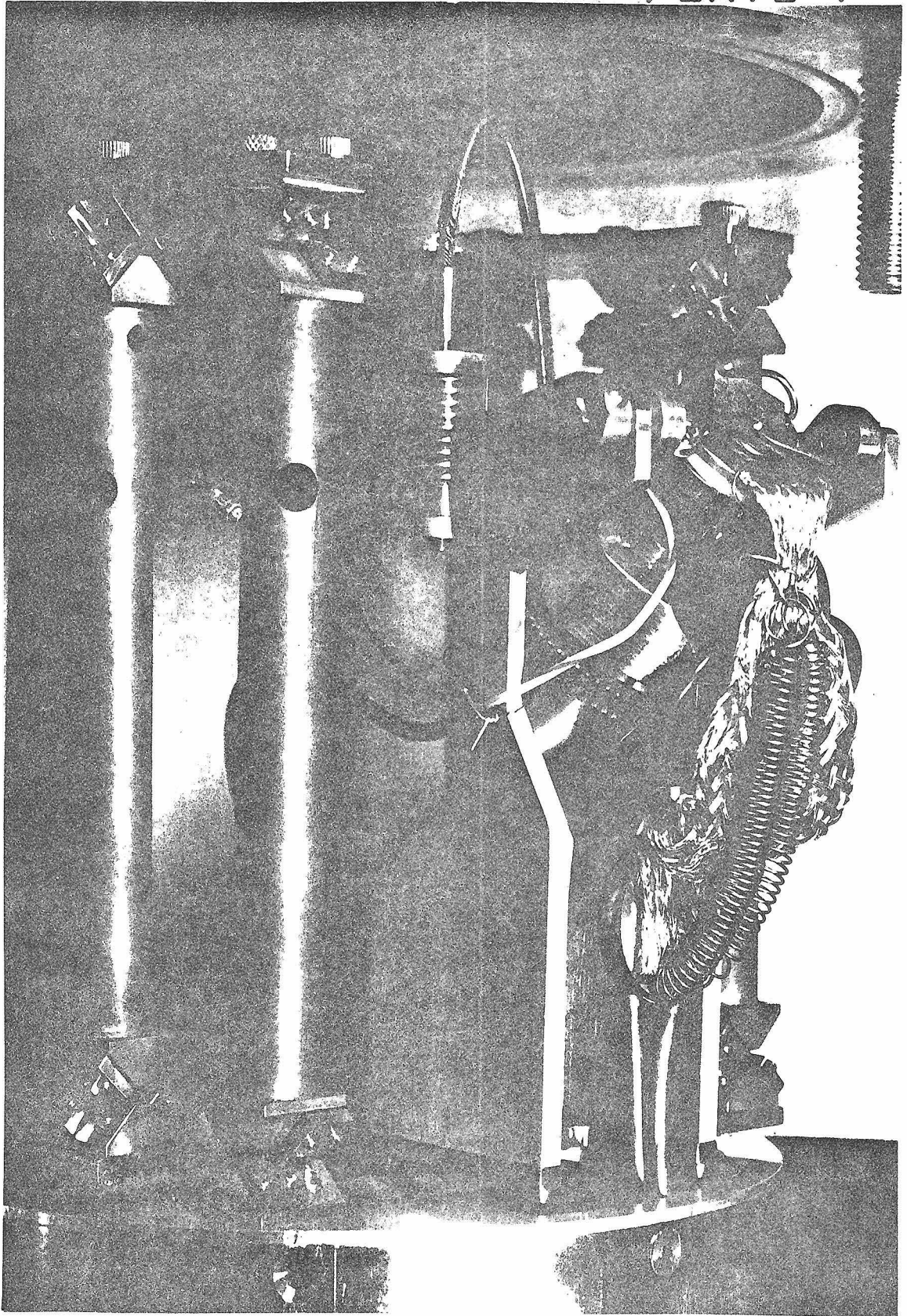
Specimen Holder. Plates 4 and 5 show the specimen removed and Plate 3 shows the holder installed in the chamber. In the chamber, the specimen could be moved in the X, Y, and Z directions and tilted up to 45° from the beam perpendicular. Next to the specimen was a small Faraday cup to measure the beam current. Translating the specimen to the extreme side moved the cup into position; the current was measured with a Keithly electrometer and was typically 5×10^{-10} amp.

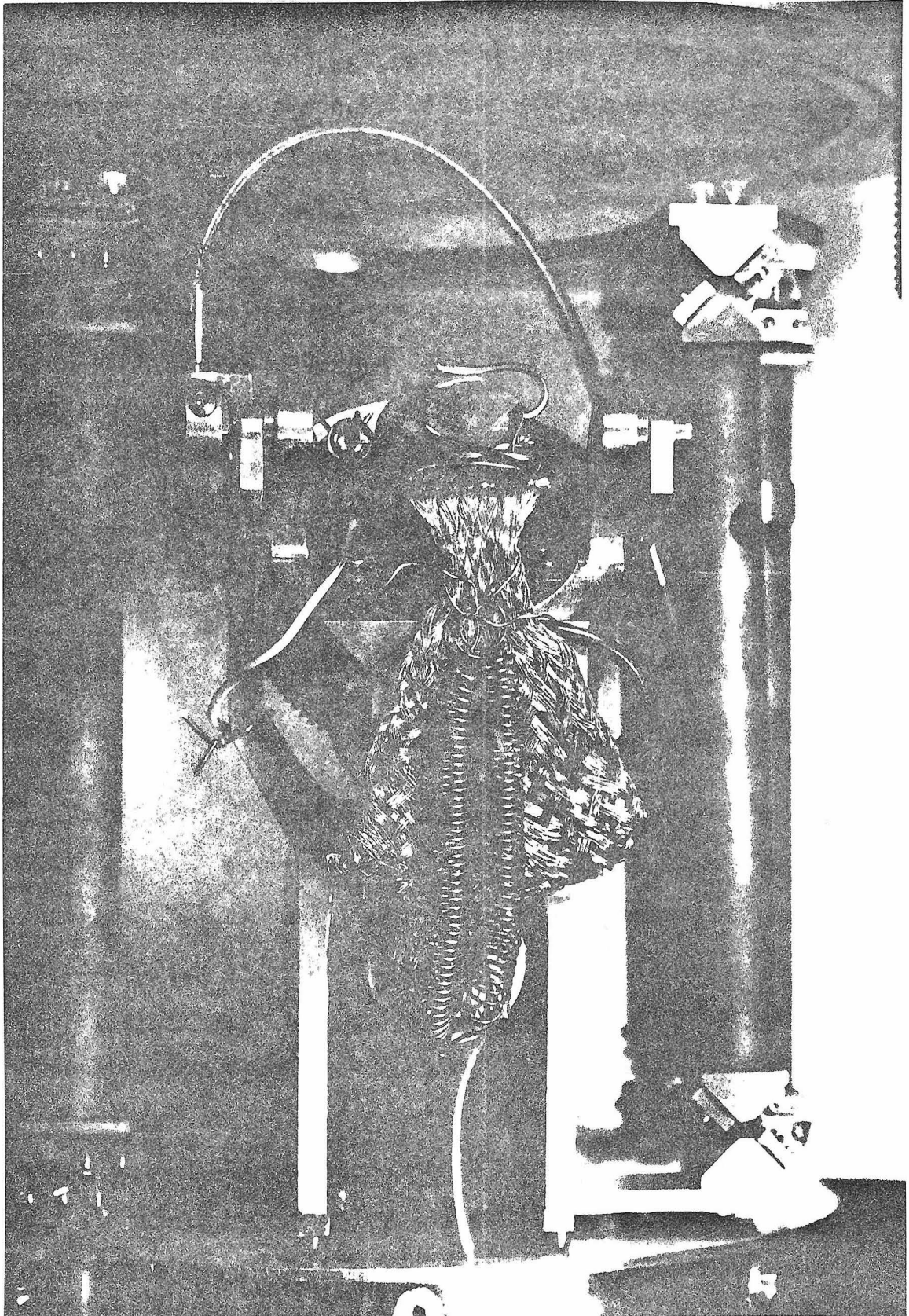
The specimen could be cooled to liquid nitrogen temperatures by pumping liquid nitrogen, under pressure (6 to 8 psi) through a small chamber. A copper braid was used to conduct the heat from the specimen to the cooled chamber. In use, the temperature dropped rapidly and in five minutes, the specimen could be cooled to

Plate 3. View of the specimen chamber looking down from the top. The one inch diameter light pipe is at 12 o'clock, the gold evaporator at 11, and the secondary electron detector at 9. The scale is about $1/3$ of actual size.

Plates 4 and 5. View of the specimen holder with specimen in place. Plate 5 shows the small Faraday cup just to the left of the specimen. The scale is about actual size.







- 150 °C. This was just about the time it took to evacuate the chamber down to a working pressure. During operation, the boiling of the liquid nitrogen caused enough vibration to degrade the 2 micron resolution. This was of no particular consequence in these experiments, but would be most undesirable in a high resolution SEM. A secure fastening for the small liquid nitrogen chamber would probably solve this problem.

Occasionally the frozen specimen would charge up under the beam. This could be cured to some extent by evaporating a thin layer of gold over the specimen. Plate 3 shows the gold evaporator in place between the secondary electron detector and large light pipe. A small cover slip was placed near the evaporator to monitor the thickness. The geometry of the system prevents getting gold at all the spots the beam can irradiate. A future design should take this into account by allowing for a greater specimen tilt.

Cathodoluminescent Detector. The light sensitive detector is an E.M.I. 9658 A photomultiplier tube with a set of seven Balzers Filtraflex filters. Figure 4 shows the percent transmission versus the wavelength for the filters. Each filter has a 60% to 70% transmission over a 100nm wide band. The transmission bands overlap

Figure 4. Transmission versus wavelength for the seven Balzers Filtraflex filters.

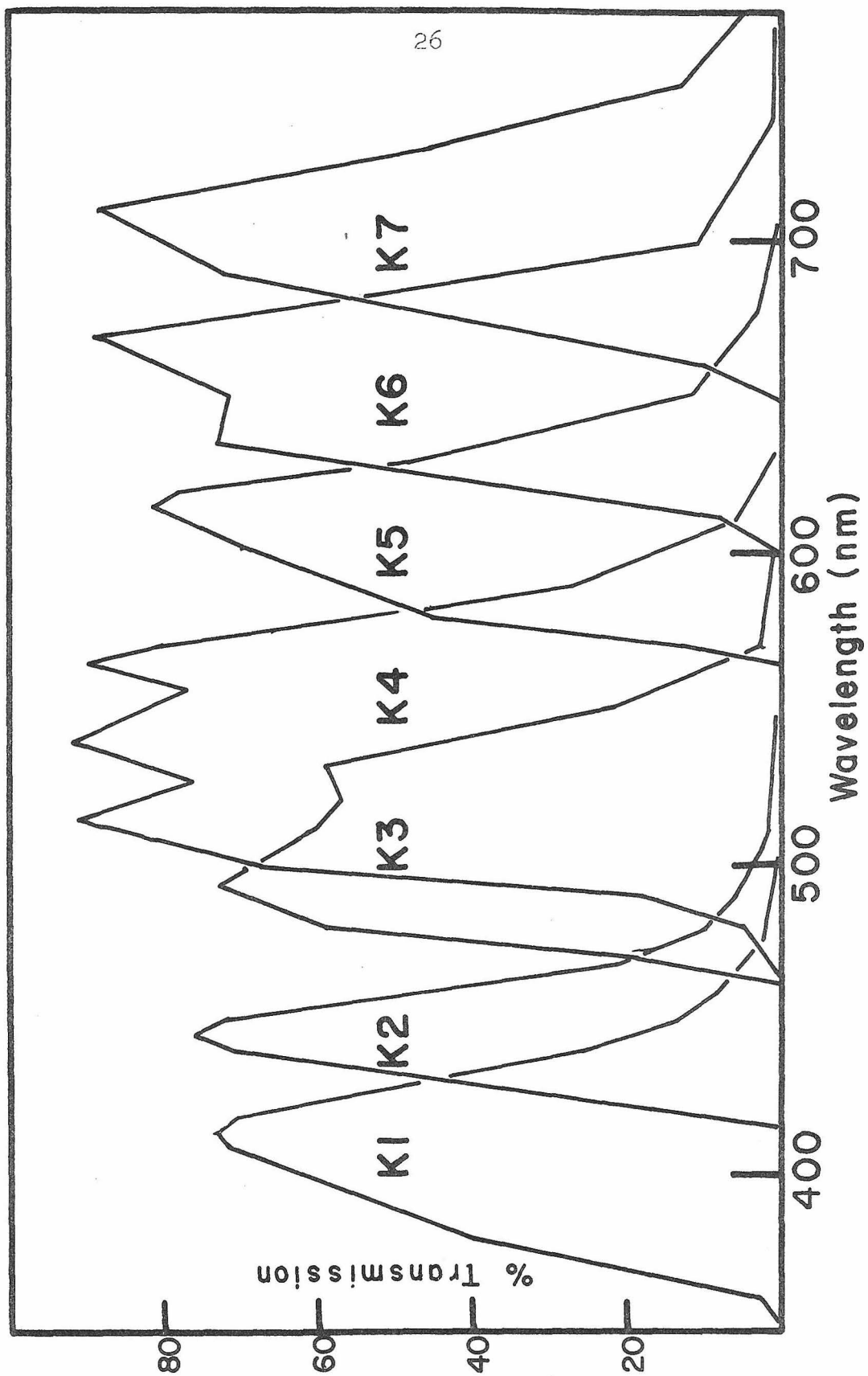
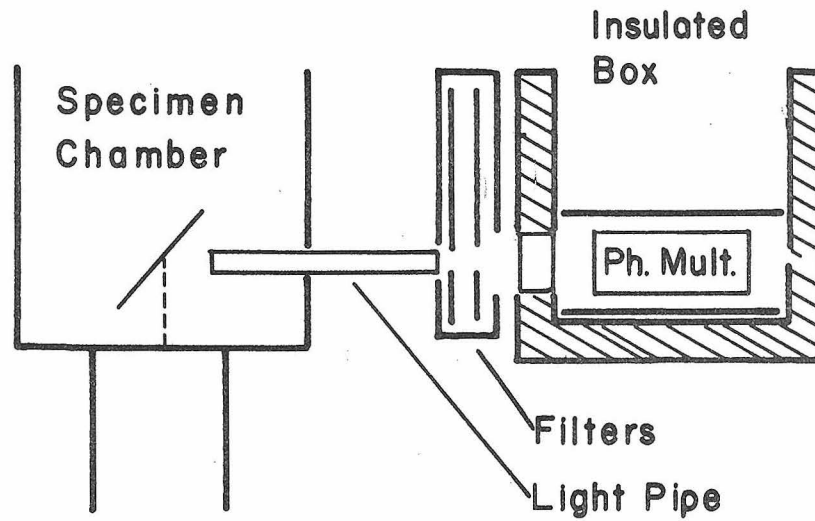


FIG 4

somewhat and are spaced evenly between 400 nm and 700 nm.

The photomultiplier tube was chosen for its high sensitivity in the red, and its low noise. The quantum efficiency of the photo cathode, according to E.M.I. literature is: 44% @ 350 nm, 20% @ 560 nm, 5% @ 740 nm, and 1% @ 820 nm. The photomultiplier tube and filters were positioned in a way to maximize light collection efficiency; this is shown in figure 5.

Light from the sample is picked up by the one inch light pipe in the specimen chamber (see also Plate 3). The light pipe brings the light to the outside by means of an "O" ring seal, and up to the filter wheels. Each filter wheel has eight positions; one wheel contains the Filtraflex filters, K1 through K7; and the other contains some neutral density and cut off filters. After filtering, the light enters a short two inch light pipe which serves to thermally isolate the photomultiplier tube from the filters. The tube is positioned in a styrofoam box. Dry ice can be added to lower the dark current down to 20 equivalent photocathode electrons per second. At room temperature, the value is 1000 times higher. Dry nitrogen gas is slowly blown over the exterior of the two inch light pipe and into the photomultiplier tube housing to prevent



Cathodoluminescence Detector

FIG 5

Figure 5. Design of the cathodoluminescence detector. A one inch diameter light pipe guides light emitted from the specimen to the filters and photomultiplier.

frost build up.

The output signal of the photomultiplier tube consists of a small fluctuating current signal of 10^{-9} amp to 10^{-6} amp. An operational amplifier transforms the current signal to a voltage signal. Appendix A gives the circuit diagram and analysis of the system.

Absolute Photometric Calibration. An absolute photometric calibration was made after the optical components were positioned.

Two samples of phosphors which had been calibrated against an N.B.S. phosphor standard were kindly donated by Dr P. N. Yocum of R.C.A.. They were $\text{Zn}_2\text{SiO}_4:\text{Mn}$ (green) and $\text{ZnCdS}:\text{Ag}:\text{Cl}$ (red). A curve was supplied with the phosphors giving the fraction of energy radiated at each wavelength, λ , per input erg of energy.

The green phosphor emitted light from 475 nm to 620 nm with most of the emission between 510 nm and 550 nm. The red phosphor emitted light in the range 550 nm to 810 nm, but data above 700 nm were not supplied. The two phosphors provided a luminous standard from 475 nm to 700 nm which was used to calibrated filters K3, K4, K5, and K6 (see figure 4). The response of the various filters is presented in Table 1.

From E.M.I. published data, one can work backward to investigate what fraction of the light

Table 1

Filter	Number of Photons Emitted per Second from the Specimen to Produce 1×10^{-6} amp of Photocurrent
K3	1.81×10^{10}
K4	0.89×10^{10}
K5	2.39×10^{10}
K6	3.53×10^{10}

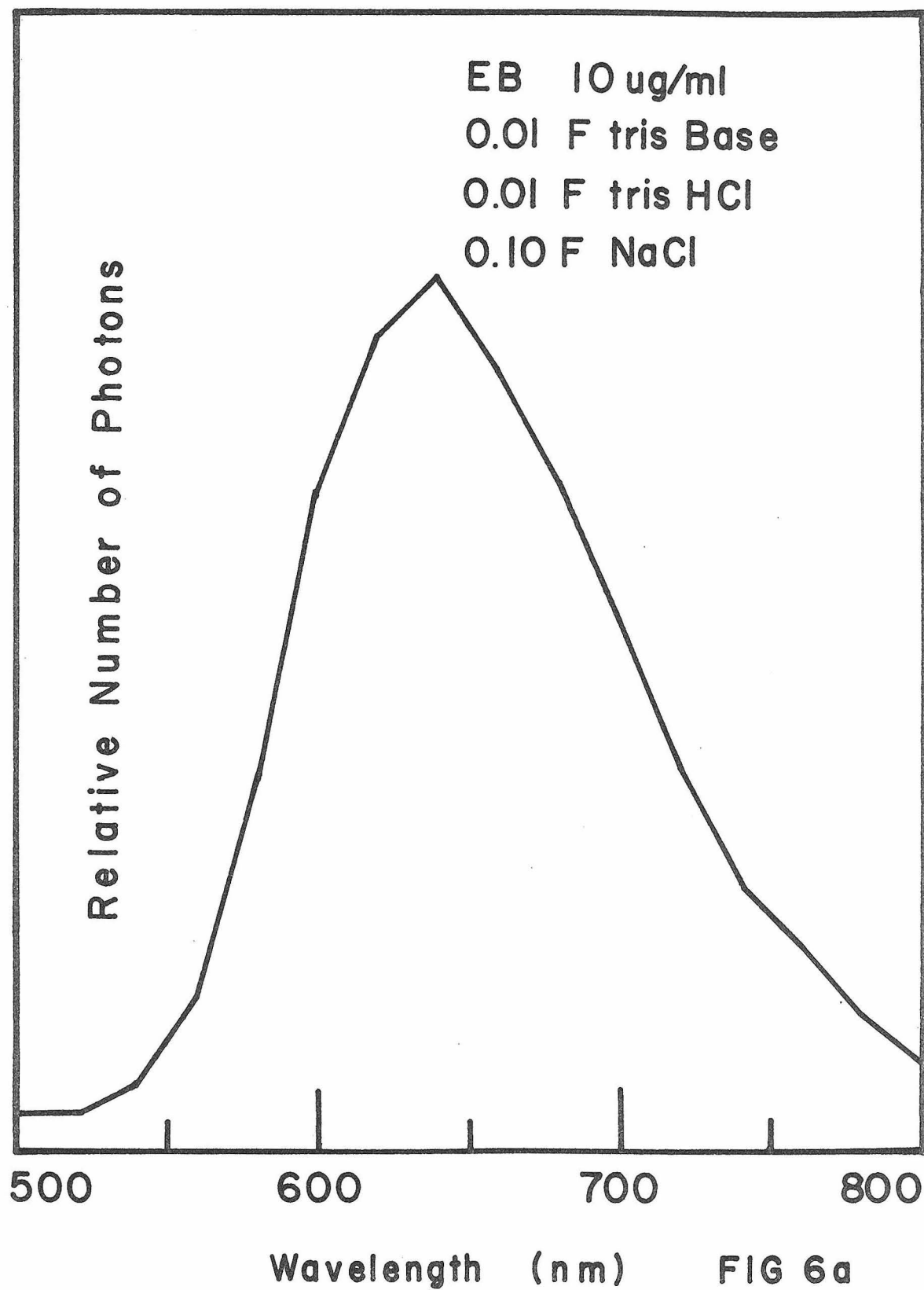
is being collected. With no filters, about 1% of the number of photons emitted by the specimen arrive at the photocathode.

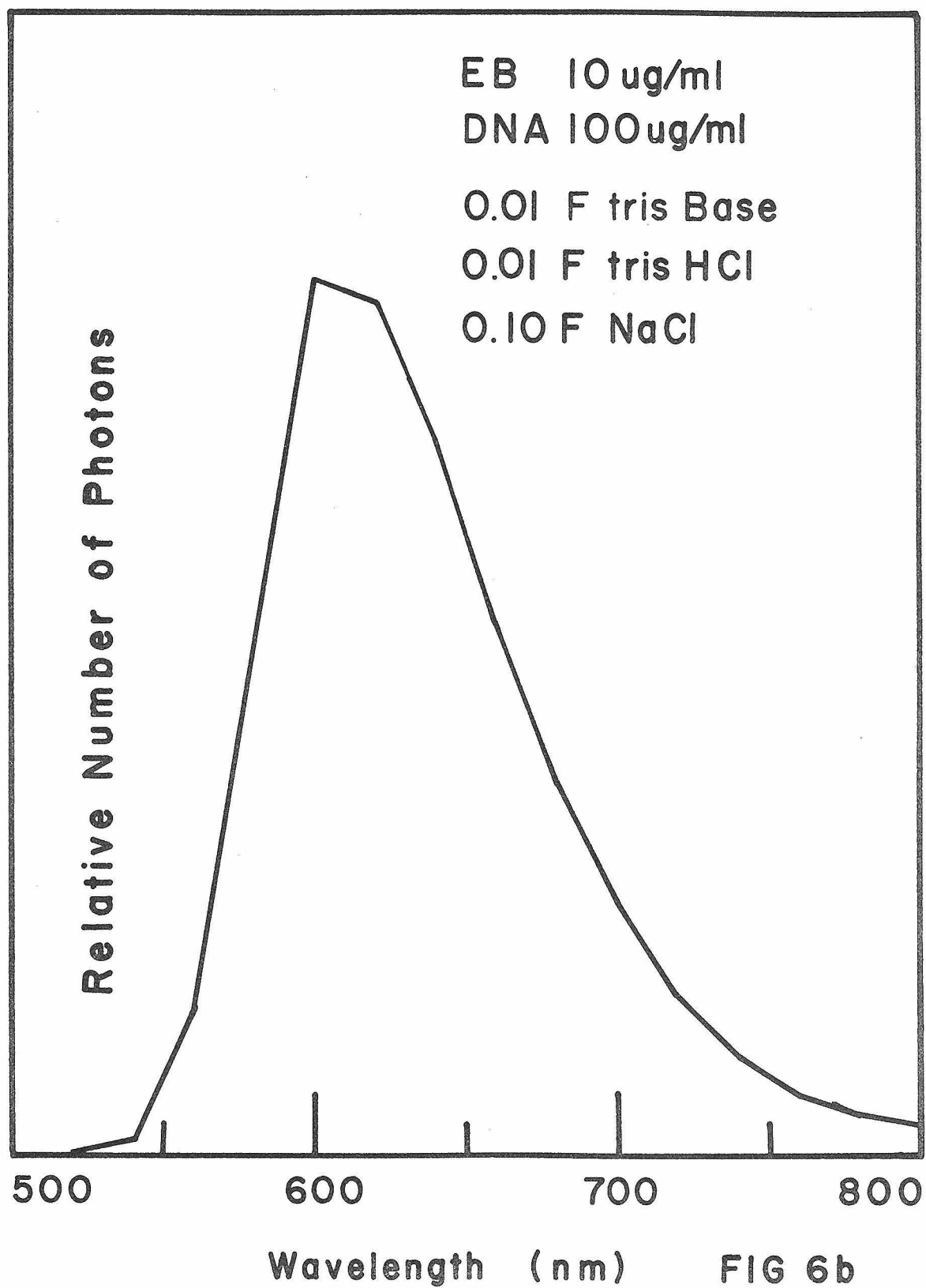
Relative Photometric Calibration of a Fluorimeter.

Early work with the red sensitive E.M.I. photomultiplier indicated that the emission from EB was centered much further into the red than reported by Le Pecq and Paoletti (6). A standard lamp was used to calibrate a grating monochromater and photomultiplier combination in order to investigate this discrepancy.

An absolute photometric calibration of a 150 watt General Electric FCS lamp was performed by the Cary Instrument Co. of Monrovia. The lamp provided a known source of energy in the wavelength region 350 nm to 550 nm, Its calibration was extended to 800nm by fitting the given output to a black body curve.

Figure 6. (a) Relative emission spectrum of ethidium bromide and (b) ethidium bromide bound to DNA (calf thymus). The fluorescence was excited by means of a medium pressure mercury arc lamp in combination with a Corning 7-37 filter.





Pivovonsky and Nagel have tabulated many black body curves (7). Using the Cary calibration data, the energy emitted at 500 nm was divided into that at 380 nm. This ratio matches the equivalent ratio for radiation from a black body at 3280°K (for a tabulation of tungsten emissivity, see ref. 8). A table of calculated lamp powers versus Cary calibration powers was made. The values agree to within 2% in the wavelength range of 340 nm to 540 nm. This technique was used to extrapolate the lamp power output data to 800 nm.

A Bausch and Lomb grating monochromator with the CL detector (E.M.I. 9658 A photomultiplier) was calibrated using this lamp.

This system was used to check the emission spectrum of EB and EB bound to DNA with UV excitation. Work with the calibrated system confirmed the filter data and in exact agreement with the emission spectra subsequently reported by Angerer and Moudrianakis (9). The emission spectrum of EB and EB bound to DNA is given in figure 6.

Specimen Preparation

To obtain the cross sections, we need to irradiate a known mass-thickness of dye. The mass-thickness of the specimen should also be less than the range of a 15 KV electron so none of the dye molecules is shielded. This range, for a sample density of 1 g/cc is on the order of 5 to 10 microns (10, 11) for such an electron.

EB-DNA. DNA would not bind EB after the DNA had been embedded so that the standard thin sectioning approach couldn't be used to prepare specimens. It was hoped that DNA embedded in a water compatible plastic such as propylene glycol monomethacrylate or durcupan* would bind EB, but it did not. Polymerization reactions also destroyed the EB, so prestained DNA couldn't be embedded and sectioned. DNA and EB solutions and gels were dried, sprayed, cut, etc., but the resulting thin films were never uniform.

Reasonable success was finally achieved by smearing a paste of DNA, EB and glycerol of known composition into shallow grooves. The technique for making the paste is as follows. 10 mg of calf thymus

* durcupan is a registered trademark of Fluka AG.,
Buchs SG/ Switzerland.

DNA was placed in a small test tube and spun dry in a clinical centrifuge to pack it down. Next, 0.050 ml of 0.01 F NH_4Ac was added, and the tube respun. After an hour or so the DNA had formed a clear gel. Glycerol, 0.050 ml, followed by EB, 2.0 mg were added. After several days, the gel was evenly stained with EB.

Shallow grooves of a known depth were prepared by vacuum coating a glass slide with 2 to 3 microns of aluminum, and then scratching grooves in the aluminum with a sharp chisel like tool. The tool removed the aluminum down to the level of the glass. The depth of the grooves was checked by interference microscopy.

A small amount of the DNA gel was placed near some grooves and the grooved surface was clamped against a siliconized slide. The gel spread and filled the grooves. This sandwich was frozen in liquid nitrogen and then pried apart. The grooved surface, filled with gel, was then placed on the specimen holder; cooling and pump down were started simultaneously.

Dansylation of polylysine. The adjunct of dansyl chloride with polylysine was chosen as the specimen to test the effectiveness of dansyl chloride bound to protein as a CL dye.

Polylysine, 12.5 mg, was dissolved in 0.58 ml of 0.02 F NaHCO_3 pH 8.0. This was then mixed with 0.58 ml

of 10% dansyl chloride in acetone (Pierce Chemical Co.). A bright yellow precipitate formed immediately which coated the walls of the test tube. The reaction mixture was shaken over the walls of the test tube every 15 minutes for a total of 2 hours at room temperature. The bright yellow material was then washed in 0.2 F NaHCO_3 and dissolved in 80% acetone. It was reprecipitated by the addition of 2 volumes of 0.2 F NaHCO_3 and centrifuged into an oily pellet in a Sorval SS-34 rotor at 10,000 rpm for 10 minutes. The bright yellow oil crystallized during storage in the freezer.

One of the small crystals was placed on the grooved aluminum and the siliconized slide was clamped against it. The sandwich was warmed to 50° C (approximately) melting the crystal. The sandwich was treated as previously described for the DNA-EB gel.

Chromatin-EB. Chromatin from rat liver was a gift from Dr Sally Elgin. It had been purified to the sucrose pellet stage (12). The pellet was resuspended in 0.01 tris pH 7 with the aid of a homogenizer. The optical density at 260 nm was measured (scattering was corrected for by plotting $\log(\text{OD})$ vs $\log \lambda$) and EB was added to P/D = 47, (47 DNA phosphates to one EB molecule). This mixture was centrifuged in a SW 50.1 rotor for 2 hours at 40,000 rpm, 4° C. A pellet of

fluorescent gel was obtained with a density of just over 1 g/cc, containing 540 ug/cc DNA (by spectrophotometry with scattering correcting). The sample was mounted as previously described.

HeLa Cell Nuclei - EB. HeLa cells were grown in suspension culture using the Dulbecco modification of Eagle's phosphate medium supplemented with 5% calf serum. Cells were spun down, resuspended in isotonic buffer, and after swelling, homogenized. Nuclei were intact and collected by centrifugation. They were washed four times by resuspending them in 2mM MgSO_4 , 5mM tris HCl, 5mM tris base, 10mM NaCl, 0.25 M sucrose, 0.3% triton X 100. Clean nuclei were then fixed in osmium tetroxide, and suspended in 5mM NaH_2PO_4 , 5mM Na_2HPO_4 , pH 7.

The amount of EB binding to osmium fixed nuclei was determined spectrophotometrically. The mass of DNA per HeLa cell nuclei was taken as 15×10^{-12} g (13). Fixed nuclei were suspended in distilled water. An aliquot was removed and the number of nuclei per ml determined by means of a cell counter. The spectra of a aliquot of EB in distilled water was taken and then 0.2 ml of suspended nuclei were added. After mixing, the nuclei were removed by means of a clinical centrifuge, and the spectrum of the supernatant was taken to determine the concentration of the remaining unbound EB.

In this experiment, under zero salt conditions, with an excess of EB, the ratio of moles DNA phosphate to moles EB bound, was 5.

Frog Red Blood Cells. Blood from the Leopard frog, Rana pipiens, was a gift from Dr Janett Trubatch. The frog blood cells were immediately washed in cold 1% sodium citrate and centrifuged. The cells were repeatedly suspended in fresh 1% sodium citrate until the supernatant was clear. They were stored in 1% sodium citrate and examined within several days.

Fluorescence Microscopy. A Zeiss fluorescence microscope was used to examine all of the previous specimens before electron microscopy. The UV source was an Osram HBO 200 watt high pressure mercury arc lamp. A BG3 excitation and 47, and -65 filters were used. The sample was excited by UV up to 350 nm and the fluorescence in the region of 470 nm to 650 nm was examined. A vertical illumination device was used to examine specimens mounted on non transparent surfaces.

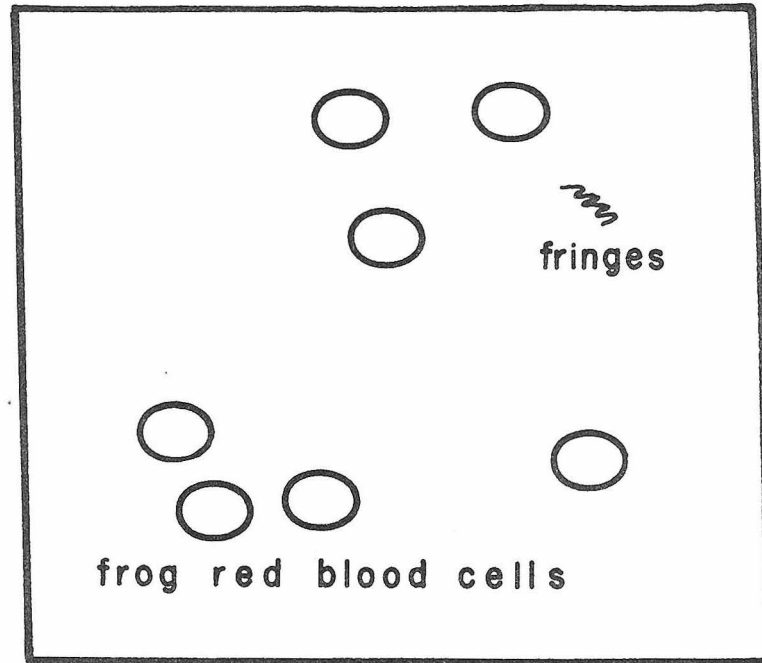
Results

Frog red blood cells were stained with EB, spread on an aluminum disk, frozen, and examined cold in the SEM. They were chosen as a specimen because of their large size and well defined nucleus. The cells are elliptical with dimensions of 30 x 15 microns, and with a nucleus of about 10 microns diameter centrally located. Plate 6 is an image obtained by collecting the secondary electrons, and plate 7 is the same field of view by cathodoluminescence. Plate 6 shows the rough surface of the aluminum sample disk as well as 7 individual and 1 clump of cells. Plate 7 shows the location of the red light emitting EB stained nuclear region of the cells.

Plate 6 also shows the extent of the vibration of the specimen stage due to the liquid nitrogen boiling. Examine the edge of the two scratches in the aluminum that run between the top center and right center of plate 6. Near the crossing of the scratches is a white object with horizontal fringes. These fringes arise from the interaction of two frequencies, the scan and the vibration. Both move the beam with respect to the sample in a repetitive manner. The depth of the fringe represents the magnitude of the vibration and the spacing is indicative of the beat frequency.

Plate 6. Secondary electron image of frog red blood cells, stained with ethidium bromide, and at liquid nitrogen temperature. The extent of the stage vibration is visible in the "fringe" (see overleaf).

Plate 7. Cathodoluminescent image of same field of view as presented in plate 6 above. Filter K6 was used (see figure 4).



Key to Plate 6

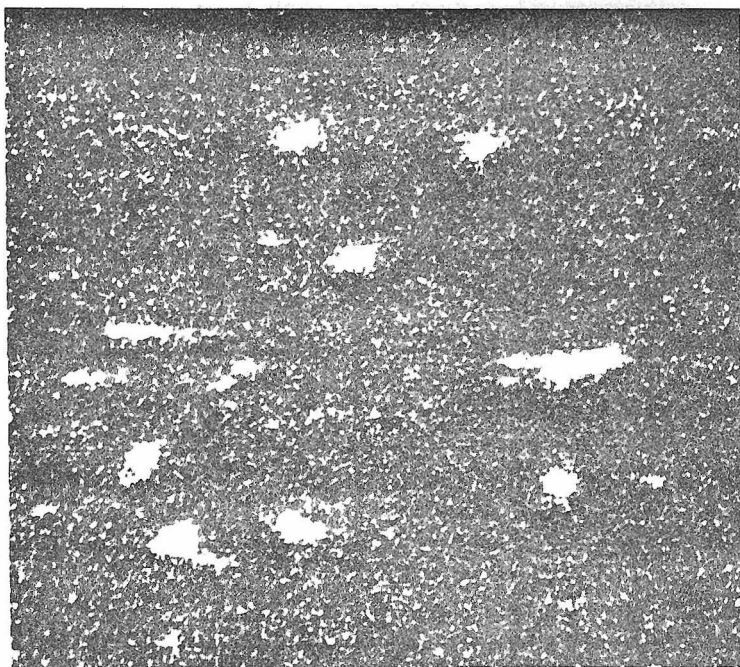
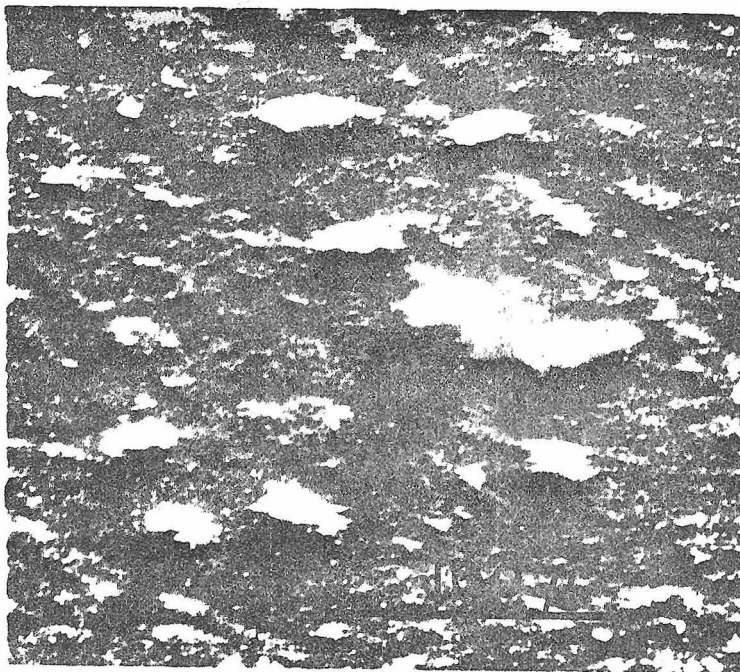


Plate 6 demonstrates a stage vibration of 5 to 10 microns.

Background Emission. The background of Plate 7 is very noisy, which indicates the photomultiplier is receiving light even though the beam is not exciting any dye. The background noise originates from four sources. They are:

1. Non specific specimen emission. This is the bluish light emitted when the electron beam strikes frozen glycerol, plastic, etc. (4, 5).
2. Scattered electrons hitting the light pipe. Photons are created in the light pipe as above, and are very efficiently collected.
3. Light from the filament. The white hot filament emits light which is scattered off the specimen.
4. Photomultiplier dark current. The photocathode emits electrons even in the absence of light.

We want to examine the contribution to the background from each of these sources. Since the light reflectivity and electron scattering properties of each specimen are somewhat different, only a rough estimate

of the magnitude of each source is possible.

The dark current contribution, source 4, is about 5×10^{-11} amp of photocurrent when the photomultiplier is cooled. For the present experiments, this represents 1% or less of the background photocurrent and can be neglected.

Table 2 gives the photocurrents obtained when the emission from a frozen layer of glycerol is examined by means of each of the filters. The photocurrents are used to calculate the relative number of photons in the band width of each filter*. This experiment measures the sum of all of the sources of background emission.

By replacing the frozen glycerol specimen with a copper screen specimen, we can measure the emission from sources 2, 3, and 4. This is possible because the metallic screen emits no light under electron bombardment (4), but does scatter light from the filament as well as electrons. These data are reported in Table 3. In addition, the accelerating voltage was turned off and the photocurrents for each filter were again measured to obtain the background emission from

* For this calculation, the spectral response of the photocathode is assumed to be as described in the E.M.I. literature.

Table 2

Background Emission from Frozen Glycerol

Filter	Photo-current amps	Relative efficiency*	Relative number of photons	Filter $\frac{1}{2}$ heights (nm) (see fig. 3)
none, HV off, fil. on	7.0×10^{-9}			
none	1.0×10^{-7}			
K1	1.5×10^{-8}	5	.3	380/440
K2	1.2×10^{-8}	3.2	.37	430/465
K3	2.5×10^{-8}	4.3	.58	475/550
K4	5.0×10^{-8}	6.4	.78	495/585
K5	4.0×10^{-9}	2.0	.2	570/635
K6	4.0×10^{-9}	1.7	.24	625/690
K7	4.0×10^{-9}	1.0	.4	675/735
dark current	7×10^{-11}			

* The "Relative efficiency" is the integral of the transmission of a filter multiplied by the average quantum efficiency of the photocathode in the appropriate wavelength range as per E.M.I. literature.

The sample is glycerol 80 microns thick, cooled to liquid nitrogen temperature. The beam current was 7×10^{-9} amp.

Table 3

Background Emission from a Copper Screen

Filter	HV on P.C.	R.N.P. I	HV off P.C.	R.N.P. II	I-II
none	3.5×10^{-7}		7.7×10^{-8}		
K1	4.2×10^{-8}	.84	3.3×10^{-9}	.06	.78
K2	3.3×10^{-8}	1.0	1.5×10^{-9}	.05	.95
K3	5.6×10^{-8}	1.3	3.4×10^{-9}	.08	1.2
K4	1.1×10^{-7}	1.6	2.0×10^{-8}	.3	1.3
K5	2.5×10^{-8}	1.2	9.0×10^{-9}	.6	.6
K6	1.5×10^{-8}	.9	1.0×10^{-8}	.6	.3
K7	1.4×10^{-8}	1.4	1.0×10^{-8}	1.0	.4

The high voltage (HV) was 15 KV. The beam current is unknown but probably 4×10^{-8} amp. The specimen was a 200 mesh copper screen mounted on an aluminum specimen stub. The relative number of photons (R.N.P.) is obtained by dividing the photocurrents (P.C.) by the relative efficiency as defined in table 2.

sources 3 and 4 alone for the copper screen. By means of these experiments, we can calculate the magnitude of all of the individual sources of background.

Source 3, the filament light, is expected to have a spectral distribution like a black body radiator. The peak of its radiation is expected to be above 800 nm, with little radiation in the blue. This is clearly demonstrated in table 3 in the column labeled "R.N.P.", "II". Here the relative number of photons increases as the wavelength increases, just as expected from a black body radiator. The photocurrent from this source is also constant i.e. it doesn't change as the beam is scanned. The magnitude of this signal will depend on the apertures used; filament location, alignment and temperature, and specimen reflectivity.

The scattering of electrons into the light pipe, source 2, and non specific sample emission, source 1, both cause blue - green emission. The light pipe is a good enough scintillator so that a CL image of the copper screen is actually possible. This CL image is in reality a reflected electron image as the copper screen produces no light under electron bombardment (4). The spectral output of the light pipe under electron bombardment is shown in table 3 under the column "I-II". Here, the photocurrent due to the filament

light is subtracted from the combined filament and light pipe signal. Most of the light is in the blue-green with a substantial tail into the red part of the spectrum. The column "Relative number of photons" in table 2 has very similar values - probably because the frozen glycerol specimen doesn't reflect much filament light into the light pipe.

The magnitude of the light pipe and non specific specimen emission background appears to be greater than the filament light background. Also, most of their light output is in the blue - green. In addition, the magnitude of the signal is dependent on beam position which is not the case for the filament light. For these reasons, a red emitting dye can be more easily detected than other shorter wavelength emission colors, all other things being equal.

In summary, there is a large fluctuating signal due to scattered electrons hitting the light pipe and non specific specimen emission. Most of the light generated is in the blue - green portion of the spectrum. Light from the filament, scattered off the specimen, is mainly in the red portion of the spectrum and doesn't fluctuate as the beam scans.

Fixation. All of the specimens used in the SEM were first examined by fluorescence. During the early

stages of investigation, it was found that glutaraldehyde fixation imparts a green fluorescence. One reference, Manger and Bessis (14), suggested that vaporized paraformaldehyde was a cathodoluminescent stain for protein. Paraformaldehyde, glutaraldehyde, and osmium tetroxide were tested on cells (Balb 3T3 cells grown in Eagle's medium were a gift from Dr J. Jordon) and DNA. Table 4 presents the data.

Table 4

Fixative	Material	Fluorescence
glutaraldehyde 3%, 0° C, 10 mM NaH ₂ PO ₄ , 10 mM Na ₂ HPO ₄ , 30 min.	cells cells after OsO ₄ fix.	bright green- yellow none
paraformaldehyde dried material with vapor, 90° C, 90 minutes	cells DNA cells after OsO ₄ fix.	bright green none none
OsO ₄ 2%, 40 mM NaH ₂ PO ₄ , 40 mM Na ₂ HPO ₄ , 0° C 60 minutes	cells	none
none	cells	none

The fluorescence was optically judged using a fluorescence microscope as previously described.

After any of the fixation procedures, the nuclei of the cells could be stained with EB. With osmium tetroxide, only the nucleus was fluorescent. For this

reason, osmium tetroxide was selected as the fixative to be used for cathodoluminescent studies.

Excitation and Destruction Cross Sections. The excitation cross section is defined by the equation

$$\sigma_{\text{ex}} = P/CI ; \quad (\text{photons } \text{\AA}^2/\text{electron}) \quad (1)$$

where P = photon current (photons per sec)

I = beam current (electrons per sec)

C = dye area concentration (number per \AA^2)

The destruction cross section is defined by the equation

$$\sigma_d = \frac{\ln(C_0) - \ln(C)}{D} ; \quad (\text{\AA}^2/\text{electron}) \quad (2)$$

where (C_0) = concentration of dye before irradiation

(C) = " " " after "

D = dose per area (electrons per \AA^2)

Figure 3 shows a block diagram of the apparatus used to measure σ_{ex} and σ_d . The beam is scanned in a long narrow raster perpendicular to and across one of the grooves. The raster size is 50×1024 . Each scan line of 50 takes 25 msec to complete. The 10 Hz cut off filter passes a signal with 100 msec or longer duration time, removing much of the noise. The signal from the photomultiplier and 10 Hz cut off filter is then

plotted on the vertical axis of an oscilloscope and the position in the 1024 side of the raster is plotted on the horizontal axis. As the beam crosses a groove filled with fluorescent dye, the signal increases and then falls back. This peak voltage (photocurrent) is used to calculate the photon current, P . D is calculated from the beam current and magnification, and the term $\ln(C_0) - \ln(C) = \ln(P/P_0)$.

The results are presented in table 5. For the EB and quinacrine, the excitation cross section is for the production of a photon in the K6 filter bandwidth, 625 nm to 690 nm. For EB, the excitation cross section for the production of any red photon (assuming the emission is that of figure 6) will be about 3 times larger than the values reported here.

The destruction cross section, σ_d , as defined, is the slope of the plot $\ln(C)$ versus the dose/ area, D . Figure 7 shows several of these plots for EB and quinacrine HCl (QHCl) with σ_d values corresponding to the various slopes. It is evident that the experimental points do not fall on a straight line, at least not until the dose is high. The values reported in table 5 correspond to the slope of the flat tail of these plots at high dose.

Figure 7. Plots of $\log_e(C)$ versus the electron dose for EB and QHCl. The upper plots are for a sample of 2 mg DNA + .05 ml 0.01 F NH_4Ac + 0.4 mg EB + 0.05 ml glycerol at liquid nitrogen temperature.

The lower plots are for 10 mg DNA and 2 mg dye, the other conditions are the same.

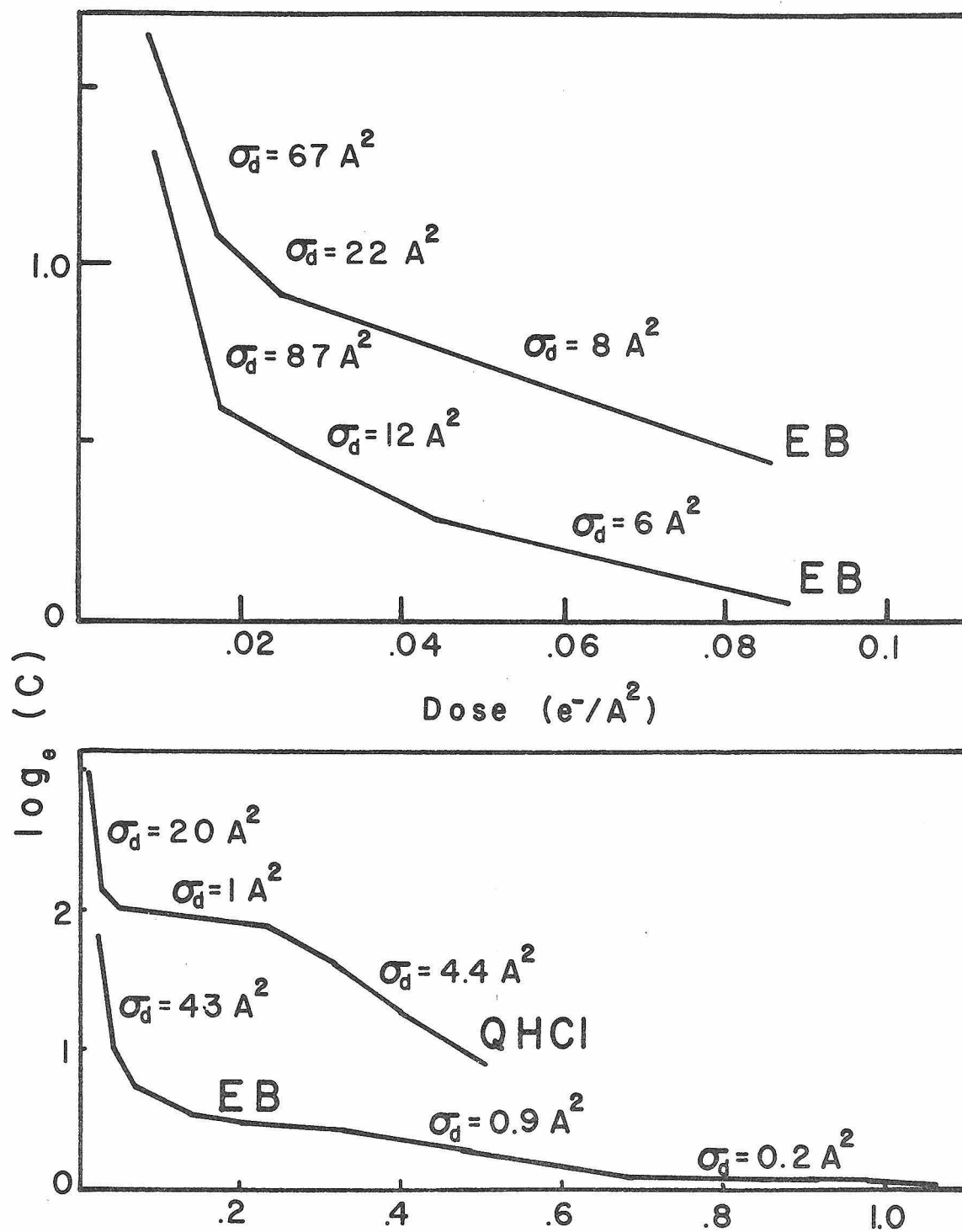


FIG 7

Table 5

Cross Sections for Excitation and Destruction
using filter K6

Sample	σ_{ex} A ²	σ_d A ²	Remarks
2 mg DNA+.05 ml NH ₄ Ac+.4 mg EB+ .05 ml glycerol, LN2 temp	.5 .35 .95	7.4 - 5.3	Several independent experiments
10 mg DNA+.05 ml NH ₄ Ac+.05 ml gly- cerol+2 mg EB, LN2 temp	.2	4.5	
Same as above + 9 mg m-Xylene diol	.3	-	It was hoped that m-Xylene diol would improve the energy transfer to EB
Chromatin-EB as previously described LN2 temp	5	17	High value of ex is probably due to energy transfer along the DNA
HeLa cell nucleus with EB, room temp	.02	-	
HeLa cell nucleus with glycerol LN2 temp	.6	-	
10 mg DNA+.05 ml NH ₄ Ac+2 mg QHCl+ .05 ml glycerol LN2 temp	.1	20	
Dansyl-polylysine LN2 temp	0		Used filter K4

DNA was from calf thymus

NH₄Ac was 0.01 M

LN2 = liquid nitrogen

Accelerating voltage = 15 KV

Discussion

The results reported in the preceding section, while approximate, are adequate to estimate the ultimate sensitivity and resolution of the cathodoluminescent mode of detecting nucleic acid - ethidium bromide complexes in the scanning electron microscope.

One estimate can be based on the background emission. We have already pointed out that a general background emission occurs from, non specific specimen emission, scattered electrons hitting the light pipe, and filament light scattering from the specimen. We can use the data in tables 1 and 2 and the cross sections in table 5 to calculate the dye area concentration, C , that is required to obtain a photocurrent equivalent to that obtained by irradiating frozen glycerol. A photocurrent of 4×10^{-9} amp with filter K6 corresponds to a specimen photon current, P , of 1.4×10^8 photons/sec by table 1. Taking $\sigma_{ex} = 0.5 \text{ \AA}^2$ and using equation 1, we find $C = 0.01$ dye molecules/ \AA^2 for EB. The excitation cross section is 5 times less for QHCl so $C = 0.05$ dye molecules for this case.

These calculations have neglected any destruction of the dye. The smaller the beam diameter, the more rapidly the dye is degraded. In fact, under high

resolution conditions (small spot size), the destruction of the dye is of major importance. Let us calculate how many dye molecules are necessary to produce say 100 recorded photons. The number of dye molecules in the irradiated area as a function of dose is given by

$$(n) = (n_0) \exp(-\sigma_d D) \quad (3)$$

(This is a theoretical expression, assuming that σ_d is constant. As already pointed out, figure 7 shows that σ_d is itself variable with dose.)

The light emission is given by

$$\int P \, dt = \int \sigma_{ex} (n) \, dD \quad (4)$$

$$= \int \sigma_{ex} (n) \exp(-\sigma_d D) \, dD \quad (5)$$

$$= \frac{\sigma_{ex} n}{\sigma_d} (1 - \exp(-\sigma_d D)) \quad (6)$$

$$\cong \frac{\sigma_{ex} n}{\sigma_d} \quad (7)$$

$$RE = (eff) \frac{\sigma_{ex} n}{\sigma_d} \quad (8)$$

RE is the number of recorded events and (eff) is the efficiency (overall system). We take $RE = 100$, $(eff) = .001$, $\sigma_{ex} = 0.5 \, A^2$, $\sigma_d = 5 \, A^2$, and calculate $n = 1 \times 10^6$ molecules of EB.

Note that this calculation assumes $\sigma_d = 5 \, A^2$.

For the first part of the decomposition curve (figure 7) the value of σ_d is still greater, and a realistic calculation of n would give a still greater value.

This is a discouraging result. Assume that there is 1 EB per 5 nucleotides. We can then detect 2.7×10^{-15} gm of DNA. It has been estimated that by fluorescence microscopy with acridine orange staining, it is possible to detect 10^{-16} to 10^{-15} gm of DNA (15).

An alternative way to look at the problem is the following. Suppose nuclear material contains DNA at a density of 1.00 g/cc. A cube containing 2.7×10^{-15} gm has dimensions 1400 Å. Thus the minimum detectable area for such a specimen would be 1400 Å x 1400 Å which is no improvement on light microscopy.

Bibliography

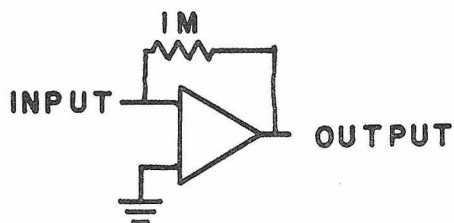
- 1) R.F.W. Pease, T.L. Hayes, Nature, 210, 1049, 1966.
- 2) T.L. Hayes, R.F.W. Pease, "Advances in Biological and Medical Physics", J. H. Lawrence and J.W. Gofman editors, Academic Press, New York, 1968.
- 3) D.A. Shaw, R.C. Wayte, P.R. Thornton, Appl. Phys. Letters, 8, 289, 1966.
- 4) J.B. Birks, W.A. Little, Nature, 174, 82, 1954.
- 5) A. Norman, M.A. Greenfield, P.M. Kratz, Nature, 171, 487, 1953.
- 6) J.B. LePecq, C. Paoletti, J. Mol. Biol., 27, 87, 1967.
- 7) M. Pivovonsky, M.R. Nagel, "Tables of Black Body Radiation Functions", Macmillan, New York, 1961.
- 8) J.C. De Vos, Physica, 20, 612, 1954.
- 9) L.M. Angerer, E.N. Moudrianakis, J. Mol. Biol., 63, 502, 1972.
- 10) J.B. Birks, "Theory and Practice of Scintillation Counting", Pergamon Press, Macmillan Co., 1964.
- 11) P.R. Thornton, "Scanning Electron Microscopy", Chapman and Hall Ltd., London, 1968.
- 12) S.C.R. Elgin, J. Bonner, Biochemistry, 9, 4440, 1970.
- 13) "Handbook of Biochemistry - Selected Data for Molecular Biology", Chemical Rubber Co., Cleveland, Ohio, 1968.
- 14) W.M. Manger, M. Bessis, "Proceedings", American Physiological Society, 13, number 3, Abstracts of papers, p 254, Aug. 1970.
- 15) T. Caspersson, S. Farber, G.E. Foley, J. Kudynowski, E.J. Modest, E. Simonsson, U. Wagh, L. Zech, Experimental Cell Research, 49, 219, 1968.

Appendix A

Photocurrent to Voltage Converter

The measurement of a non fluctuating photocurrent of the order of 10^{-8} amp is readily made with an electrometer voltmeter and a large resistance. This system responds slowly though because of capacitive effects (RC is large). It is desirable to be able to make a measurement of the photocurrent as rapidly as possible. One way of speeding this up is to add an operational amplifier at the photomultiplier output.

The operational amplifier used in practice has a voltage gain of 100,000 for the normal input (+), and -100,000 for the inverting input (-). It is connected to the photomultiplier anode directly as follows.



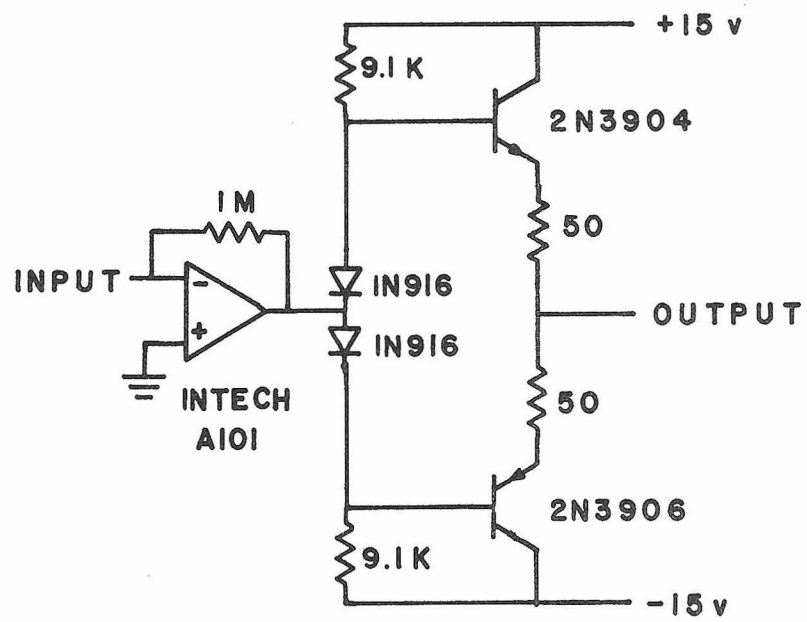
The input resistance of this device is 10^{11} ohms.
consider what happens as a pulse of electrons arrive

from the photomultiplier anode. The voltage at the (-) input starts to go negative, the output of the amplifier rapidly goes very positive due to the gain of -100,000. The pulse of electrons is then removed through the 10^6 ohm feedback resistor leaving the (-) input at zero volts and thusly returning the output to zero volts also. In practice, the high gain of the amplifier keeps the (-) input at a potential very near zero volts, appearing to the photomultiplier anode as a virtual ground. One microampere of photocurrent will cause the output of the amplifier to go to +1.0 volts.

This device speeds up the measurement because the time constant of the circuit, RC, is greatly reduced.

In operation, the amplifiers sometimes burnt out because of the high current output required when excessive capacitance is connected across the output of the amplifier. The circuit shown below increases the effective maximum output current of the amplifier and was used in all experiments.

The circuit will convert current to voltage at the ratio of 1 volt output/ 1 microampere input. Its measured frequency response using a sine wave current input is from DC to 200 K Hz.



Photocurrent to voltage converter

Part 2

PARTIAL DENATURATION MAPS OF LAMBDA DNA
USING METHYLMERCURIC HYDROXIDE

64
Introduction

Methylmercuric hydroxide (mmh) is known to react with DNA (1,2,3). It reacts with thymine at the N-3 position (1), and with guanine at the N-1 site. Because both of these sites are used to form Watson-Crick hydrogen bonds in native DNA, mmh reaction causes denaturation. Since the equilibrium constant for reaction with thymine is about 10 times greater than that for reaction with guanine, and since adenine-thymine (AT) base pairs are weaker than guanine-cytosine (GC) base pairs (4), it is expected and found, that mmh denatures AT rich DNA's more readily than GC rich DNA's (2).

It was hoped to use mmh to selectively denature the AT rich regions of a DNA. The location of these regions could be mapped by electron microscopy. By varying the mmh concentration, the AT composition along a DNA could be obtained.

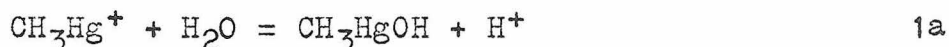
Inman obtained data of this nature by thermally denaturing DNA in the presence of formaldehyde (5). He observed denatured regions in lambda DNA at various temperatures. These AT rich regions were not uniquely located however; the number of denatured loops he observed, and the fraction denatured, varied from molecule to molecule. We assumed the variability in Inman's method was caused by the nonselective melting

behavior of DNA. Mmh, because of its preferential binding to thymine, was expected to increase the selectivity of denaturation over thermal denaturation alone.

The results obtained show that mmh denatures DNA as selectively as heat and formaldehyde. The difference, if any, is small and does not allow any significant improvement over Inman's technique.

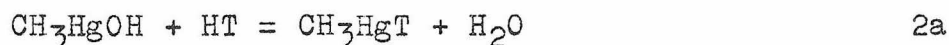
In order to predict how mmh reacts with DNA, we examine the reactions of mmh with individual nucleosides and, using this data, calculate how the simultaneous DNA denaturation and reaction with mmh should occur. Most of this information is reported in Gruenwedel and Davidson (2), but is given here for completeness.

Mmh reacts readily with nitrogen bases, EDTA, and chloride ion. These materials were avoided in all of these experiments. In addition, the compound CH_3HgOH which reacts with thymine and guanine, is ionized at low pH's according to the equilibrium

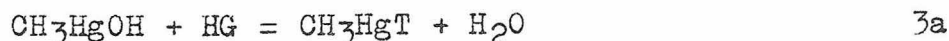


$$\frac{(\text{CH}_3\text{HgOH})(\text{H}^+)}{(\text{CH}_3\text{Hg}^+)} = 10^{-4.58} \quad (25^\circ \text{C}, \mu = 0.1\text{M NaClO}_4) \quad 1b$$

All of the reported experiments are at a pH between 7 and 8, where the mercury is predominantly in the form CH_3HgOH . In this form it can react at the N(3)-H bond of thymine, HT, and at the N(1)-H bond of guanine, HG, by the following equilibria:



$$\frac{(\text{CH}_3\text{HgT})}{(\text{CH}_3\text{HgOH})(\text{HT})} = 10^{4.35} = K_T \quad 2b$$



$$\frac{(\text{CH}_3\text{HgG})}{(\text{CH}_3\text{HgOH})(\text{HG})} = 10^{3.4} = K_G \quad 3b$$

There are other reactive sites, but under the pH conditions of these experiments (pH 7 to pH 8), no significant further mmh binding occurs (see ref. 2).

In native DNA, the mmh binding sites are used for Watson-Crick hydrogen bonding. Denaturation then, is a prerequisite for mmh binding. The equilibrium equation for the denaturation of j base pairs, fj of which are GC base pairs, is:

$$\begin{aligned} (AT)_{(1-f)j} (GC)_{fj} &= \\ &= (A_{(1-f)j} + T_{(1-f)j} + G_{fj} + C_{fj}) \end{aligned} \quad 4a$$

We wish to formulate the equilibrium constant for this cooperative transition when it occurs within a DNA molecule (not unzipping from the end), forming a looped structure. The formation of an internal loop loses an additional stacking energy interaction relative to unzipping from the end and is therefore thermodynamically more unfavorable.

Let a_N , a_{DU} , and a_{DM} represent the thermodynamic activity of a native, a denatured unmercurated, and a denatured mercurated DNA segment of length j , respectively. Also, let s_{AT} be the equilibrium constant for the formation of an AT base pair which is at the junction of a helical and denatured region. Let ks_{AT} represent the equivalent equilibrium constant for a GC base pair;

k is greater than 1 as GC base pairs are more stable than AT base pairs. Crothers, Kallenback, and Zimm (6) estimate $k = 5.3$. The equilibrium equation associated with equation 4a is:

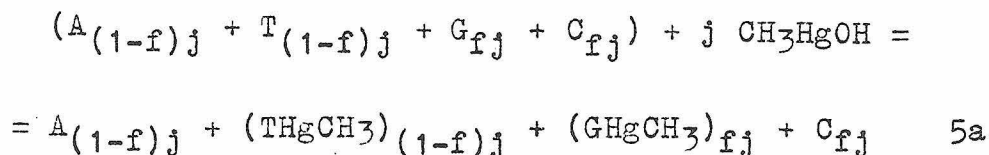
$$\frac{a_{DU}}{a_N} = (1/k s_{AT})^{fj} (1/s_{AT})^{(1-f)j} \frac{\sigma}{j^{3/2}} \quad 4b$$

$$= (1/k)^{fj} (1/s_{AT})^j \frac{\sigma}{j^{3/2}} \quad 4c$$

The first two terms of equation 4c represent the equilibrium constant for DNA denaturation when it occurs by unzipping from the end. In the last term, $j^{-3/2}$ represents the statistical unfavorability of an internal denatured loop (Jacobson, Stockmeyer ref. 7), and the loss of the extra stacking energy, σ . Crothers and Zimm (8) estimate $\sigma = 10^{-4}$.

We wish to write the equation for simultaneous denaturation and mercuration. We assume the reaction of mmh with the denatured bases is the same as for monomeric bases (equations 2 and 3). Also, we restrict ourselves to conditions where the mmh concentration is high enough so that most denatured T and G bases react with mmh. We also only look at the point of 50% denaturation where we will apply the final equation.

The equilibrium reaction of denatured DNA with mmh is then:

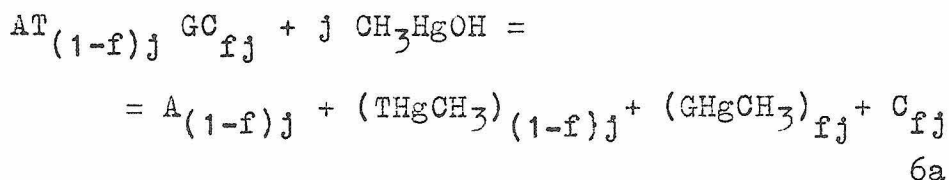


$$\frac{a_{DM}}{a_{DU}} = K_T^{(1-f)j} K_G^{fj} (\text{CH}_3\text{HgOH})^j \quad 5b$$

If we let $K_T = r K_G$ (equations 2b and 3b) with $r = 10^{0.9}$ then equation 5b may be rewritten as:

$$\frac{a_{DM}}{a_{DU}} = \frac{K_T^j}{r^f} (\text{CH}_3\text{HgOH})^j \quad 5c$$

The simultaneous mercuration and denaturation can be represented by combining equations 4 and 5.



$$\frac{a_{DM}}{a_N} = \frac{K_T^j (\text{CH}_3\text{HgOH})^j}{r^f} \left(\frac{1}{k}\right)^j \left(\frac{1}{s_{AT}}\right)^j \frac{\sigma}{j^{3/2}} \quad 6b$$

$$= \frac{\sigma}{j^{3/2}} \left[\frac{(\text{CH}_3\text{HgOH}) K_T}{(rk)^f s_{AT}} \right]^j \quad 6c$$

The constant, s_{AT} , is evaluated in Gruenwedel and Davidson (2) for 25° C.

$$s_{AT} = 7.7$$

The other constants are:

$$K_T/K_G = r = 10^{4.3}/10^{3.4} = 10^{0.9}$$

$$s_{GC}/s_{AT} = k = 5.3 = 10^{0.72}$$

$$r k = 42 = 10^{1.62}$$

$$K_T/s_{AT} = 10^{4.3}/10^{0.9} = 10^{3.4}$$

Equation 6c may then be rewritten as:

$$\frac{a_{DM}}{a_N} = \frac{10^{-4}}{j^{3/2}} \left[\frac{(\text{CH}_3\text{HgOH}) 10^{3.4}}{(10^{1.62})^f} \right]^j \quad 6d$$

This equation is qualitatively useful to calculate the mmh concentration required to denature a DNA. Since no intermediate states of denaturation were considered in its formulation, it is not expected to predict the mmh melting curve of DNA.

In order to see why mmh was expected to be a very selective denaturant, let us evaluate the mmh concentration using this equation for a typical case, $j = 1000$ base pairs, $f = 0.50$ GC, at 50% denaturation where $a_{DM}/a_N = 1.0$. Putting in these values in equation 6d yields:

$$\frac{10^{-4}}{10^{4.5}} \left[\frac{(\text{CH}_3\text{HgOH}) 10^{3.4}}{10^{0.81}} \right]^{1000} = 1$$

$$\begin{aligned}
 (\text{CH}_3\text{HgOH}) &= (10^{9.5})^{(1/1000)} 10^{-2.59} = \\
 &= 1.022 \times 2.57 \times 10^{-3} = 2.63 \times 10^{-3} \text{ F}
 \end{aligned}$$

The ratio $a_{\text{DM}}/a_{\text{N}}$ is very sensitive to the mmh concentration. If the amount of mmh is now increased by 1%, the ratio $a_{\text{DM}}/a_{\text{N}}$ changes by $(1.01)^{1000} = 2.1 \times 10^4$. Simultaneously, the difference in mmh concentration needed to denature 0% and 100% GC DNA is the factor $k_r = 42$.

This large GC dependence led to the expectation that mmh could be used as a selective denaturant for AT rich regions.

Experimental

Lambda c₂₆ phage were grown and collected by standard procedures. The phage were banded in a CsCl density gradient, removed by dripping, and dialyzed into 0.01 F NaH₂PO₄, 0.01 F Na₂HPO₄, 0.01 F MgCl₂. The DNA from the phage was released just prior to the experiment by heating to 60° C for 15 minutes (9).

The DNA was mounted for electron microscopy by the basic protein film technique. The mmh was in the spreading solution only. This solution was prepared by addition of the following, in the order given.

Stock Solution	Amount	Final Concentration
7.5 F KAc	0.066 ml	0.5 F
0.01 F Phosphate Buffer *	0.724 ml	0.007 F
0.01 F mmh	0.10 ml	0.001 F
DNA	0.01 ml	0.5 ug/ml
1 mg/ml cyt c	0.10 ml	0.10 mg/ml

* 0.005 F NaH₂PO₄ and 0.005 F Na₂HPO₄

The solution volume was always 1.0 ml, the buffer volume was increased or decreased as DNA or mmh volumes were changed. When the cytochrome c was added, the solution was spread onto 0.5 F KAc immediately. This was done to minimize the reaction of mmh with the basic protein. The film was picked up on Parlodian

covered grids. The grids were shadowed at an 8:1 angle with Pt:Pd and examined in the electron microscope. The denatured regions appeared as loops and were easily visible by the technique. Representative spread out molecules were photographed, and enlargements made. A map measurer was then used to measure the location and size of each denatured loop.

Methylmercuric hydroxide ("Panogen concentrate; 21.5% mercury") was kindly donated by the Agricultural Division, Morton Chemical Company, Woodstock, Ill. The 0.01 F stock solution was made by dilution with distilled water.

Data

The total length of the partially denatured molecules, l , is less than the normal double stranded length, $L = 14.95$ u for lambda c_{26} DNA. Single stranded DNA mounted under these salt conditions was known to be shorter than corresponding double strand molecules. For the purposes of mapping, it was desired to have a length of double strand DNA melt into the same length of single strand DNA. To do this, a computer converted the raw data in the following manner:

let lss = length of single strand in a molecule
(only one branch of a loop is measured)

lds = length of double strand DNA per
molecule

$$l = lss + lds$$

For each molecule, a single strand expansion factor, F , was calculated by the formula

$$F = \frac{L - l + lss}{lss} = \frac{L - lds}{lss}$$

Each length of single stranded DNA in that particular molecule was expanded by the factor, F . This procedure results in all molecules having the same length. The value of F varies from molecule to molecule; this most likely results from fluctuations in amount of non observed denatured regions.

The half of lambda DNA with the most denaturation was oriented to the right, the molecules were individually plotted, and a group histogram plotted. Also of interest is the fraction and standard deviation of looping, and the number of loops per molecule.

Results

Denaturation maps of lambda c₂₆ DNA, mounted in the presence of 8.0×10^{-4} F mmh and 1.25×10^{-3} F mmh are presented in figures 1a and 2a respectively. Figures 1b and 2b are histograms of the respective groups of molecules.

The data presented in these figures may be used to examine the selectivity of mmh denaturation. Our theoretical arguments predict that the number of denatured regions per molecule, the fraction of denatured material per molecule, and the location of these regions should be the same from molecule to molecule at any given mmh concentration. Table 1 presents the number

Table 1

mmh concentration	average number of denatured regions per molecule	fraction denatured
8.0×10^{-4} F	4.1 ± 1.6	$0.051 \pm .019$
1.25×10^{-3} F	6.0 ± 1.3	$0.103 \pm .031$
Inman's formaldehyde	10.5 ± 3.8	$0.11 \pm ?$

error limits are one standard deviation

of denatured regions per molecule and the fraction denatured per molecule for the two experiments as well one of Inman's experiments (5) for comparison. In

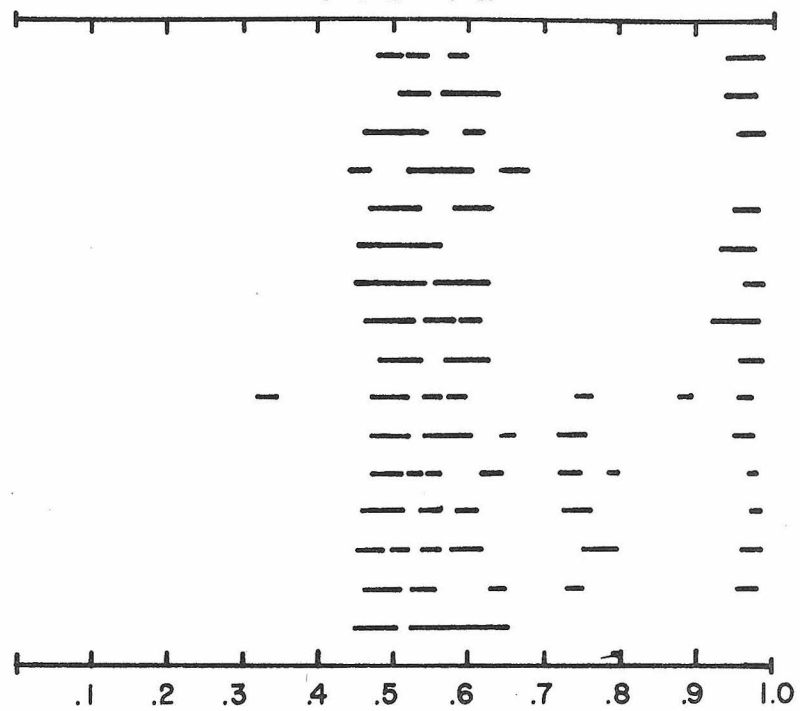
Figure 1. (a) Denaturation map of lambda c₂₆ DNA mounted in the presence of 8.0×10^{-4} F mmh. The dark bars indicate the portions of the molecules that are denatured.

(b) A histogram of the denatured regions in (a).

Figure 2. (a) Denaturation map of lambda c₂₆ DNA mounted in the presence of 1.25×10^{-3} F mmh. The dark bars indicate the portions of the molecules that are denatured.

(b) A histogram of the denatured regions in (a).

78
FIG 1a



Fractional Length of λ
 $\text{mmh} = 8.0 \times 10^{-4} \text{ M}$

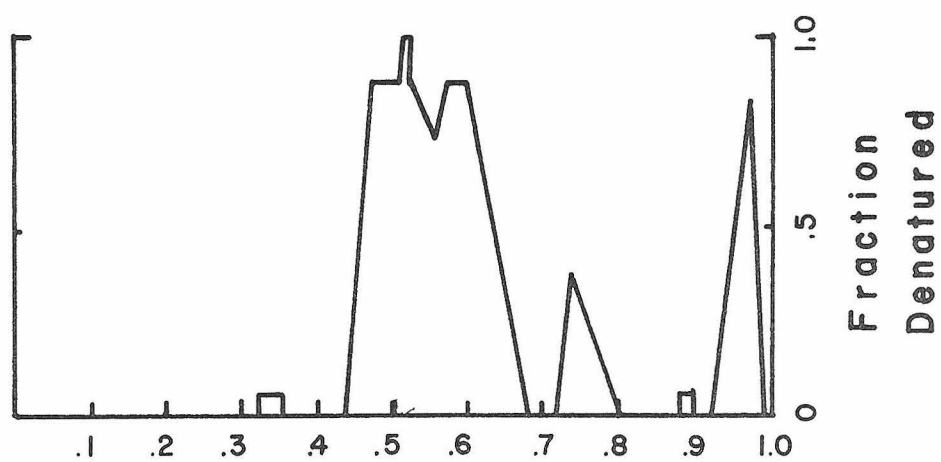
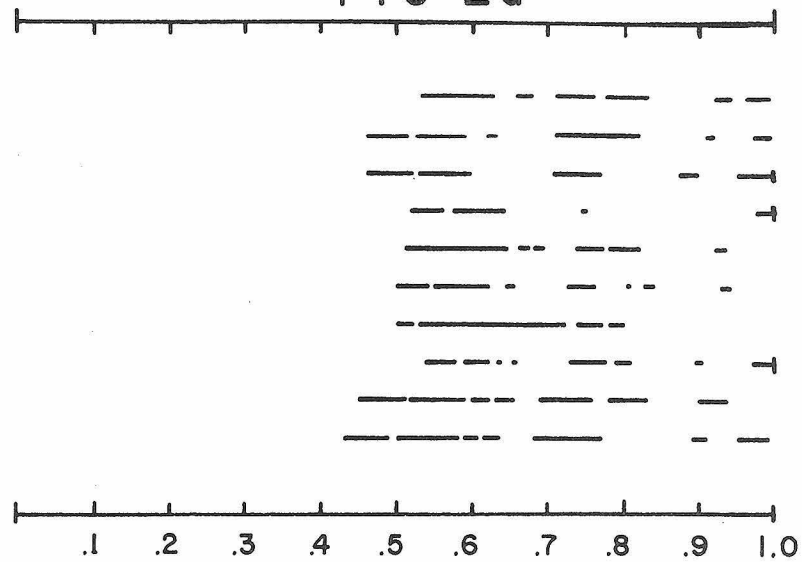


FIG 1b

FIG 2a



Fractional Length of λ

$$mmh = 1.25 \times 10^{-3} M$$

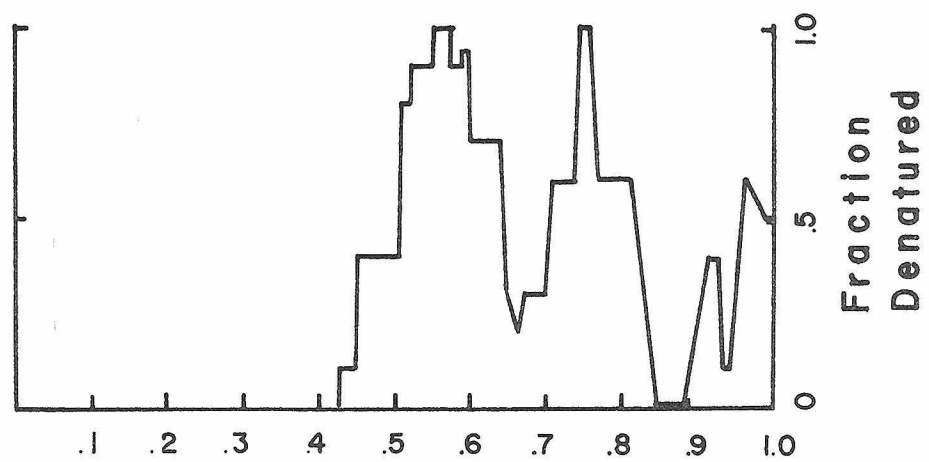


FIG 2b

general, the data in table 1 imply a much greater fluctuation in denaturation than theoretically expected. The standard deviation of the fraction denatured per molecule as well as the number of loops per molecule is on the order of 20% to 30%.

In the right most denatured region in figures 1b and 2b, the amount of denatured material is greater in figure 1b where the mmh concentration is lower. This is contrary to prediction and the behavior of the other denatured regions. This strange behavior also occurred in Inman's work (see ref. 5, p 112, fig. 6).

The mmh concentrations used with respect to figures 1 and 2 have been experimentally found (2) to $\frac{1}{2}$ denature a DNA of base composition of 40% and 48% GC. As lambda c₂₆ DNA is 50% GC, both of these mmh concentrations should cause over $\frac{1}{2}$ of the molecule to denature. This is obviously not the case.

The large fluctuations mentioned above might arise during the addition of cytochrome c and the subsequent spreading. Here, the chemical equilibrium is clearly disturbed. Two ideas were tested in order to prevent the system from fluctuating. The simplest idea was to add mmh to the hypophase. Unfortunately, the basic protein won't form a film under these conditions and no DNA could be visualized on the grids. The other

idea was to fix the DNA loop structure with formaldehyde, then add cytochrome c and spread.

The latter idea was tested spectrophotometrically. Calf thymus DNA was 15% denatured * (by hyperchromicity) by the slow addition of mmh while stirring. A small amount of formaldehyde was then added to make the solution 0.028% in formaldehyde. This increased the amount of denaturation up to 25% (it took several hours for the plateau value to be reached). The addition then of either NH_4Ac (reacts with mmh and formaldehyde) or NaCl (reacts with mmh only) caused immediate renaturation. These data imply that the reaction of formaldehyde with DNA is reversible and would not fix the DNA as originally hoped.

* The DNA could be denatured up to 35% and it would still be capable of almost complete renaturation by removal of mmh.

Discussion

The deviations from theory prevent using equation 6d to determine the GC composition. There is however, still a way to experimentally calibrate the system.

Lambda DNA is sheared into small pieces and banded in cesium formate. Here, Schmid and Hearst (10) have found that the diffusion and density spreading may be separated and, the separation on the basis of base composition is large. The data from such an experiment allow a table of mass of DNA versus %GC to be constructed. If, under a certain mmh concentration, 10% of the DNA is denatured, we assume that we have denatured the most AT rich regions. The %GC value at which 10% by mass is more AT rich, may easily be found from the table of mass DNA versus %GC.

Even with the system calibrated, it is doubtful that the base composition analysis would be carried out to an accuracy greater than $\pm 5\%$ GC. This can be understood by examining the qualitative behavior of equation 6d. In a previous example, we calculated the mmh concentration for $j = 1000$ base pairs, and $f = .5$. We found

$$\frac{(\text{CH}_3\text{HgOH}) 10^{3.4}}{10^{1.62f}} = (10^{9.5})^{(1/1000)} = 1.022$$

If j is allowed to increase, the term a_{DM}/a_N in equation 6d also increases. The $j^{3/2}$ in the denominator is negligible in comparison. This implies that if the stretch of $f = .5$ DNA is larger than $j = 1000$, the DNA will further denature. We may ask, how must f change such that

$$\frac{2.63 \times 10^{-3} F 10^{3.4}}{10^{1.62f}} = 1.00$$

so that denaturing another base is no longer thermodynamically favorable. The result is

$$\frac{10^{1.62 f}}{10^{.81}} = 1.022; f = .512$$

This implies that the GC content must increase by over 1% in order to halt further denaturation. For smaller values of j , the problem is worse, i. e. a much larger value of f is needed to halt further denaturation.

In addition to this effect, the actual base sequence must play an important role. As a denatured loop grows it crosses many potential energy wells corresponding to AT rich regions. There is probably no large potential well so the final size of the denatured region is somewhat random. This and the previously mentioned effects are probably responsible for the fluctuations observed.

This technique can be compared to that of

Inman's (5). The parameter used to compare the two is the "average number of denatured loops per molecule" data in table 1. The standard deviations in this value are assumed to represent the extent of uncertainty in the method. In both Inman's and this work, the standard deviation is about 30% to 40% so the techniques would have to be judged about equal by this criterion. The fluctuations in "average number of denatured regions per molecule" appear to be less in Inman's recent work but since the complete data isn't given, no comparison is possible. The location of the AT rich regions is the same by the two techniques.

Since the technique offered no inherent advantages over the Inman technique, it was not further pursued.

Bibliography

- 1) R. B. Simpson, J. Am. Chem. Soc., 86, 2059 (1964).
- 2) D. W. Gruenwedel, N. Davidson, J. Mol. Biol. 21, 129 (1966).
- 3) D. W. Gruenwedel, N. Davidson, Biopolymers 5, 847, (1967).
- 4) J. Marmur, P. Doty, J. Mol. Biol., 5, 109 (1962).
- 5) R. B. Inman, J. Mol. Biol., 28, 106 (1967).
- 6) D. M. Crothers, N. R. Kallenback, B. H. Zimm, J. Mol. Biol., 11, 802 (1965).
- 7) H. Jacobson, W. Stockmeter, J. Chem. Phys., 18, 1600 (1950).
- 8) D. M. Crothers, B. H. Zimm, J. Mol. Biol., 9, 1 (1964).
- 9) R. Husky, Thesis, California Institute of Technology, (1968).
- 10) C. Schmid, J. Hearst, Biopolymers, 11, 1913, 1972.

Proposition 1

Interaction of Electrophoresing DNA
with Neutral Macromolecules

Electrophoresis and sedimentation in the ultracentrifuge of macromolecules are two powerful tools for the investigation of the properties of large molecules, as well as for separations of components on the basis of size, shape, and charge. These techniques are particularly useful because the behavior of molecules can be calculated as well as experimentally investigated.

This proposition proposes a model for the interaction of charged nucleic acids with neutral polymers in an electrophoresis system. One of the predictions of the model is that nucleic acids of any arbitrary size may be electrophoretically separated.

Theory

Before proposing a model for the interaction of DNA and neutral polymers, let us briefly examine the behavior of DNA in centrifugal and electric fields.

In the ultracentrifuge, DNA is subjected to an acceleration force which causes it to move through the solvent. The acceleration force is balanced against one of friction as the molecules move. At a given centrifugal field, the force on the molecule due to the field is proportional to the mass of the molecule. The retarding force due to friction is approximately proportional to the square root of the mass (1). This behavior is to be expected if we examine the conformation of native DNA in solution.

The shape assumed by DNA, a somewhat flexible macromolecule, is that described by a random walk in 3 dimensions (2). The size of each step or segment in this random walk is determined by the stiffness of the polymer (3). For native DNA, this value has been found to be 717 A (4) to 1000 A. A large DNA in solution, having many of these freely jointed segments, resembles a loosely wound ball of yarn. Although the density of DNA by mass at the center is not high, the segments are close enough such that the solvent in the interior and the DNA move together during sedimentation (5). Thus

the frictional coefficient for sedimentation resembles that for a sphere which obeys Stoke's law and (2,3) is:

$$f_0 \propto R \propto \text{mass of DNA}$$

1

where f_0 is the friction coefficient for a sphere, R the radius which is proportional to the square root of the mass of DNA. In practice, DNA's of various molecular weights move in a centrifugal field as predicted and separation on this basis is quite feasible.

At first thought, electrophoresis of DNA would appear analogous to sedimentation. The driving force is again proportional to the mass (since the number of negative charges is proportional to the mass). It would also appear that the frictional coefficient would have the same dependence as shown in equation 1. This however is not the case. In fact it has been shown experimentally (6) that the electrophoretic mobility is not a function of the molecular weight for native DNA. This, incidentally, is what would be expected to occur for sedimentation too if DNA molecules were "free draining" instead of trapping and moving solvent with them. Let us examine now, why in the case of electrophoresis, is the DNA random coil "free draining".

The DNA backbone is composed at neutral pH's of negatively charged phosphate groups, one for every

330 daltons of molecular weight. Bound to these negative charges are positive ions from the solvent. The positive layer attracts negative ions and so forth. As the distance from the negative phosphate backbone increases, we find positive, negative, positive, ..., etc. layers of ions, each layer more loosely bound and more randomly composed than the proceeding layer. During electrophoresis, the loosely held positive ions move in the opposite direction to the DNA. This effect essentially makes the DNA molecule "free draining" and explains the lack of molecular weight dependence. There is no bulk solvent movement as in sedimentation, and each segment of the DNA experiences the electric field and friction independently of the others.

There is however a technique in which macromolecules are electrophoresed through a gel matrix. Here, as molecular size increases as with DNA, mobility decreases as it becomes more difficult to creep through the gel. The relationship between the pore size of the gel, and the number of fibers per unit volume (gel concentration) has been mathmatically (7,8) and experimentally determined (9). The relationship between the pore size, p , and the gel concentration, T is:

$$p \propto \sqrt{T}$$

For agar at 2.5% concentration, the pore size is about 0.035 μ (9). For spherical proteins, where $\log R$ is proportional to \log (molecular weight), Ferguson (10) found that the electrophoretic mobility of the protein was inversely proportional to the \log (molecular weight) and for any particular specie

$$\log M = \log M_0 - K_r T \quad 3$$

where M is the mobility in the gel
 M_0 is the mobility free (no gel)
 T is the concentration of the gel in percent
 K_r is the retardation coefficient

Gel electrophoresis of DNA has been performed by many investigators, (11, 12, 13, review on gel electrophoresis, 14) who ingeneral find that the expected dependence of \log (molecular weight) and mobility (10) does not hold for DNA of a molecular weight greater than 10^6 . In fact the mobilities of 2×10^6 and 10^8 molecular weight native DNA's are the same in a 2.5% gel (11).

The lack of dependence of the mobility on molecular weight can perhaps best be understood if we examine the conformation of a DNA of molecular weight 10^8 and compare this to the 0.035 μ pore size for a 2.5% gel (9). The most readily calculated parameter of intrest is the radius of gyration, R_g

$$R_g = (\sigma)^{\frac{1}{2}} l / (6)^{\frac{1}{2}} \quad 4$$

where σ is the number of statistical segments and l is the length of a statistical segment (assume $l = 1000 \text{ \AA}$). Taking one micron of native DNA to have a molecular weight of 2×10^6 , a molecular weight of 10^8 has $\sigma = 500$ and $R_g = 0.91 \text{ u}$. A DNA of 10^6 molecular weight would have an $R_g = 0.091 \text{ u}$.

It is clear that a sphere of radius 0.91 u will not enter a gel of pore size 0.035 u . What apparently happens is that the DNA snakes its way through the gel instead of traveling through in its spherical conformation (13, 15). With the spherical conformation lost, the expected molecular weight dependence of the mobility disappears also.

Without going into the theory of gelation (2), it seems impossible to create a pure gel with a pure gel with a pore size of one or two microns so equation 3 would apply for a 10^8 molecular weight DNA with presently available materials. It might be possible to pour a very dilute solution of agarose over a matrix of commercially available spherical agarose beads to obtain a mixed gel with large pores, but this has never been tried. In any event, let us examine how DNA and individual agarose or poly vinyl alcohol (PVA) molecules would interact in an electrophoretic system.

Introduction to the Proposed Model

Let us assume that all the segments of a random coil molecule are randomly distributed within its radius of gyration. Using the equation derived in reference (16) for the partition coefficient of spheres going into a network of fibers, we can calculate if a spherical molecule of PVA will be able to penetrate the DNA random coil. If the PVA molecule won't penetrate, the model presumes it is dragged along (with a friction coefficient as per equation 1) by the electrophoresing DNA until it is removed by lateral diffusion. For the purposes of this model, it is assumed that the rate of lateral diffusion of PVA is independent of the forward velocity of the electrophoresing DNA.

Calculations for the Proposed Model

The equation of Giddings, Kucera, Russel, and Meyers (16) equates the partitioning, K , of a spherical molecule of diameter L_0 between the open solvent and a network of random fibers of diameter l_0 and length per unit volume, h . The relationship is:

$$K = (1/f') \exp(-\pi h(L_0 + l_0)^2/4) \quad 5$$

where f' is the porosity. For DNA, l_0 will be very small compared to the diameter of the PVA molecule and can

be neglected, also the interior of the molecule is so dilute that $f' = 1$ so we can rewrite equation 5 as:

$$K = \exp(-\pi h L_0^2 / 4) \quad (6)$$

If K is small, no penetration of a PVA molecule of diameter L_0 is possible into a DNA with h cm of fiber per cm^3 .

For a DNA of molecular weight 10^8 , 50 u long, the volume occupied by the DNA is assumed to be

$$(4\pi/3)R_g^3 = (4\pi/3)(9.1 \times 10^{-5} \text{cm})^3 = 4 \times 10^{-12} \text{cm}^3 \quad (7)$$

Thus h can be calculated as

$$h = \frac{50 \times 10^{-4} \text{cm}}{4 \times 10^{-12} \text{cm}^3} = 12 \times 10^8 \text{cm/cm}^3 \quad (8)$$

and finally, rewriting equation (6)

$$K = \exp(-37.7 \times 10^8 \text{cm}^{-2} L_0^2 / 4) = \exp(-10^9 L_0^2 \text{cm}^{-2}) \quad (9)$$

Now a minimum L_0 can be calculated so that we get no penetration, $K < 1$. This occurs when

$$L_0^2 > 10^{-9} \text{cm}^2 \text{ or } L_0 > 3 \times 10^{-5} \text{cm} \quad (10)$$

Finally, we can calculate what molecular weight PVA is necessary i.e. has an $R_g = 1500 \text{ \AA} = 3 \times 10^{-5} / 2$;

$R_g^2 = 2\sigma l^2/6$ for PVA (see ref. 2, p. 415 or ref. 5, p. 156) $l = 1.54 \text{ \AA}$, the carbon - carbon bond length and σ is the number of carbon - carbon bonds,

$$R_g^2 = 2.25 \times 10^6 \text{ \AA}^2 = 2.3 \text{ \AA}^2/3 ; \sigma = 3 \times 10^6 \quad (11)$$

Each monomer has two carbon - carbon bonds ($-\text{CH}_2\text{CHOH}-$), so 1.5×10^6 monomers of molecular weight 44. The molecular weight of the PVA is then

$$44 \times 1.5 \times 10^6 = 70 \times 10^6 \quad (12)$$

Equation one shows that the density of segments within R_g , h , is even greater for smaller DNA's (the volume $R_g^3 \propto \text{mass}^{3/2}$). Thus within R_g for any smaller DNA, no PVA of molecular weight 70×10^6 can penetrate.

Since the PVA molecule is excluded from the interior of smaller DNA's also, we can write the rate of encountering PVA molecules, k_e , for any smaller DNA as:

$$k_e = u \pi R_g^2 (\text{PVA}) \quad (13)$$

In order to calculate the net amount of PVA on a DNA we compare the rate of encounter, k_e , with the rate of loss, k_l . The time for a PVA molecule to diffuse a distance R_g is given by

$$t = R_g^2 / D_{\text{pva}} \quad (14)$$

where D_{pva} is the diffusion constant of the PVA molecule. The rate of loss of PVA from an electrophoresing DNA is then calculated to be

$$k_1 = \# / t = \# D_{pva} / R_g^2 \quad (15)$$

where $\#$ is the number of PVA molecules on a DNA. At steady state, $k_e = k_1$ and

$$u R_g^2(PVA) = \# D_{pva} / R_g^2 \quad (16)$$

$$\# = u \pi R_g^4(PVA) / D_{pva} \quad (17)$$

Equation 17 predicts that the number of PVA molecules dragged along through the solvent will be proportional to the square of the molecular weight of the DNA. If enough molecules of PVA are encountered, to alter the friction coefficient, larger DNA's will migrate slower than smaller DNA's.

Table one and figure one show the expected behavior of DNA of various molecular weights with PVA of molecular weight 7×10^7 .

The predicted behavior is that very small DNA's can migrate through the PVA with no retardation. For very large DNA's, the interior is so dilute and the pore size so large that PVA can pass through with no interaction and again no retardation. DNA's of molecular

Table I

Interaction of Electrophoresing
DNA and PVA


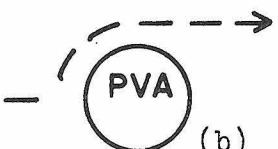
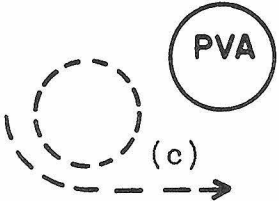
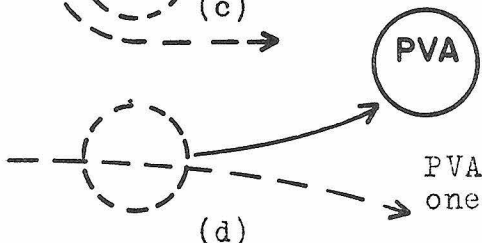

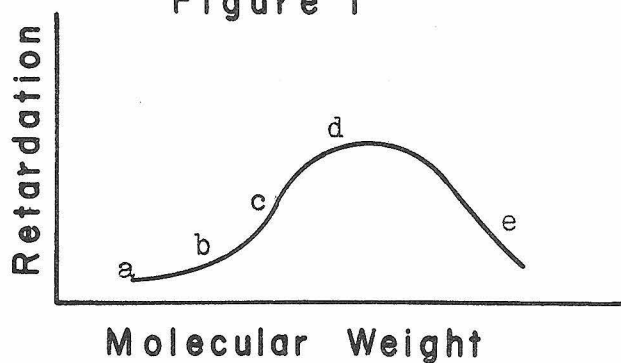
<u>DNA Molecular Weight</u>		<u>Comment</u>
less than 180 A length	 (a)	diffuses through the PVA
10^4 to 10^7	 (b)	must pass around the PVA
7×10^7	 (c)	both molecules move
10^8	 (d)	PVA has to diffuse one micron laterally
10^{10}	 (e)	interior of the DNA is so dilute no interaction occurs

Figure I



weight 10^4 to 10^8 will interact with the PVA with the prediction that larger DNA will migrate **slower**. Although the model was proposed for PVA and DNA, it is not clear whether or not that particular system would work. The problem with PVA is that as a free coil in solution, it is very compact. This means that the amount of friction due to dragging a PVA molecule through the solvent is small; simultaneously, a large mass of PVA is required to obtain a large number of molecules of PVA to interact with the DNA. The amount of PVA required can be estimated as follows. The diffusion constant of a PVA molecule with an R_g of 1.5×10^{-5} cm is 2.2×10^{-8} cm²/sec (see ref. 5, eq. 21-30). We next calculate approximately how long it would take to diffuse 0.91 μ , the radius of a DNA of molecular weight 10^8 .

$$\begin{aligned} t &= \overline{x^2}/D_{\text{pva}} = (9.1 \times 10^{-5} \text{ cm})^2 / 2.2 \times 10^{-8} = \\ &= 0.4 \text{ sec} \end{aligned} \quad (18)$$

Next we ask, what volume of solution is swept out by an electrophoresing DNA molecule of $R_g = 0.91 \mu$? At a reasonable field of 5 volts/cm, the linear velocity of the DNA is 10.8 μ /sec (ref. 6) and the volume swept per second

$$\begin{aligned} \text{Vol.} &= 10.8 \times 10^{-4} \text{ cm/sec } \pi (9.1 \times 10^{-5} \text{ cm})^2 \\ &= 2.75 \times 10^{-11} \text{ cc/sec} \end{aligned} \quad (19)$$

To have one molecule of PVA on the DNA we require that one molecule is encountered in the time it takes to diffuse off (see eq. 17). One PVA must be encountered every 0.4 sec or there must be one PVA in the volume $0.4 \times 2.75 \times 10^{-11} \text{ cc} = 10^{-11} \text{ cc}$. The mass per liter is then

$$\frac{1000 \text{ cc}}{10^{-11} \text{ cc}} \frac{7 \times 10^7 \text{ g/mole}}{6 \times 10^{23} \text{ molecules/mole}} = .01 \text{ g} \quad (20)$$

The calculation does not show how much this one molecule of PVA causes the DNA molecule to slow down. We can estimate how many are necessary to show a reasonable retarding effect by calculating the friction coefficient for electrophoresing DNA and comparing this value with the corresponding friction coefficient for sedimentation of the PVA molecule.

The friction coefficient, f , of electrophoresing DNA may be calculated from the relationship

$$u = Z/f \quad (21)$$

where u is the mobility of native DNA, $2.1 \times 10^{-4} \text{ cm}^2 \text{ volt}^{-1} \text{ sec}^{-1}$ (6) and Z is the charge. Since cations bind tightly to DNA, the charge is not simply the number of phosphate groups, but more like 20% of that value under the conditions of electrophoresis. By

taking Z equal to the number of phosphates, a maximum friction coefficient is obtained which is (using mks units)

$$\begin{aligned}
 1 \text{ segment} &= 1000 \text{ \AA of DNA} = 300 \text{ base pairs} = \\
 &= 600 \text{ phosphates} = 600 \times 1.6 \times 10^{-19} \text{ coul} = \\
 &= 9.6 \times 10^{-17} \text{ coul} \\
 u &= 2.1 \times 10^{-8} \text{ m}^2 \text{ volt}^{-1} \text{ sec}^{-1} \text{ at } 100 \text{ volts/m}
 \end{aligned} \tag{22}$$

The force on a segment, F, is given by

$$\begin{aligned}
 F &= qE = 9.6 \times 10^{-17} \text{ coul } 100 \text{ volt m}^{-1} \\
 &= 9.6 \times 10^{-15} \text{ newtons}
 \end{aligned} \tag{23}$$

Now by equation 21, the friction coefficient for one segment is:

$$\begin{aligned}
 f &= F/u = \frac{9.6 \times 10^{-15} \text{ newtons}}{2.1 \times 10^{-8} \text{ m}^2 \text{ volt}^{-1} \text{ sec}^{-1}} \\
 &= 4.6 \times 10^{-7} \text{ newton sec/m}
 \end{aligned} \tag{24}$$

Since there is no molecular weight dependence in free electrophoresis, the friction coefficient is proportional to the mass, so for a DNA of molecular weight 10^8 with 500 segments, the friction coefficient is:

$$f = 500 \times 4.6 \times 10^{-7} \text{ newton sec/m} = 2.3 \times 10^{-4} \frac{\text{newton sec}}{\text{m}} \tag{25}$$

Now we can compare this value to that of one PVA

molecule with $R_g = 1.5 \times 10^{-5}$ cm which has a friction coefficient that can be calculated by Stoke's law, $f = 6\pi\eta R$ where $R = 0.665 R_g$ (ref. 5, p. 362)

$$\begin{aligned} f &= 6\pi\eta R = 6 \cdot 0.01(\text{dyne sec/cm}) \cdot 0.665 (1.5 \times 10^{-5} \text{cm}) \\ &= 1.88 \times 10^{-5} \text{ dyne sec/cm} = 1.88 \times 10^{-9} \text{ newton sec/m} \end{aligned} \quad (26)$$

This friction coefficient is about 10^5 times smaller than the maximum friction coefficient calculated for the DNA molecule. For the friction due to PVA to equal that of the DNA we would need (by equation 20)

$$0.01 \text{ g/l} \times 10^5 = 1000 \text{ g/l of PVA} \quad (27)$$

This is clearly too much to consider dissolving in one liter of solution. Dextran seems to be a reasonable candidate (17, 18). It can be obtained in high molecular weights (19, p. IV - 111) with R_g on the order of 2300 Å (17). The most economical particles in terms of weight to friction coefficient (large radius of gyration), would be stiff rod like molecules. Of all polymeric molecules reported in the literature surveyed (2, 5, 18, 19), the stiffest rod like molecule mentioned was collagen. Although charged, its isoelectric point lies near neutrality (20). It might be quite useful depending on how DNA interacts with it.

Proposed Experiments

It is proposed to test the model by using a sucrose stablized electrophoresis column as previously described (6) with an added neutral polymer such as PVA, dextran, agarose, or collagen at its isoelectric point. The solubility of these materials is the only remaining question left to answer before the experiment can be more quantitatively described and results predicted.

Bibliography

- 1) J. G. Kirkwood, J. Riseman, J. Chem. Phys., 16, 565, 1948.
- 2) P. J. Flory, "Principles of Polymer Chemistry", Cornell University Press, Ithica, New York 1953.
- 3) W. Kuhn, Kolloid Z., 76, 258, 1936.
W. Kuhn, Kolloid Z., 87, 3, 1939.
- 4) J. Hearst, W. H. Stockmayer, J. Chem. Phys., 37, 1425, 1962.
- 5) C. Tanford, "Physical Chemistry of Macromolecules", J. Wiley, New York 1961.
- 6) B. M. Olivera, P. Baine, N. Davidson, Biopolymers, 2, 245, 1964.
- 7) A. G. Ogston, Trans. Faraday Soc., 54, 1745, 1958.
- 8) D. Rodbard, A. Chrambach, Proc. Nat. Acad. Sci., 65, 970, 1970.
- 9) G. K. Ackers, R. L. Steere, Biochim. Biophys. Acta, 59, 137, 1962.
- 10) K. A. Ferfuson, Metabolism, 13, 985, 1964.
- 11) C. W. Dingman, M. P. Fisher, T. Kakefuda, Biochemistry, 11, 1242, 1972.
- 12) C. W. Dingman, A. C. Peacock, Biochemistry, 7, 659, 1968.
- 13) M. P. Fisher, C. W. Dingman, Biochemistry, 10, 1895, 1971.
- 14) A. Chrambach, D. Rodbard, Science, 172, 440, 1971.
- 15) C. Aaij, P. Borst, Biochim. Biophys. Acta, 269, 192, 1972.
- 16) J. C. Giddings, E. Kucera, C. P. Russel, M. N. Meyers, J. Chem. Phys., 13, 4397, 1968.
- 17) E. Antonini, L. Bellelli, M. R. Bruzzesi, A. Caputo, E. Chiancone, A. Rossi-Fanelli, Biopolymers, 2, 27, 1964.

- 18) "Encyclopedia of Polymer Science and Technology",
Vol. 4, 814, N. M. Bikales ed., Wiley, 1971.
- 19) "Polymer Handbook", J. Brandrup, E. H. Immergut
editors, Interscience, Wiley, New York, 1966.
- 20) "Electrophoresis of Proteins", H. A. Abramson,
L. S. Mayer, M. H. Gorin, Reinhold Publishing
Corp., New York, 1942.

Proposition 2

On the Mechanism of Electrophoretic
Migration of DNA in Gels

Electrophoresis has proven to be a powerful tool in the characterization of macromolecules. Unfortunately, this elegant and simple method has been rather useless for the separation of high molecular weight DNA's according to molecular weight. The reasons why electrophoresis fails to differentiate DNA's on the basis of their molecular weights are discussed. Experiments are proposed to test a current model of this behavior.

It has been shown experimentally that there is no molecular weight dependence of the electrophoretic mobility in aqueous solution with no supporting gel for native DNA (1). This is to be expected theoretically because loosely bound counter ions of the negatively charged DNA migrate, in the electric field, in the opposite direction to the DNA. This effect causes the DNA molecule to be "free draining" and the electrophoretic friction coefficient becomes proportional to the mass. Since the force for electrophoresis is also proportional to the mass, the resultant electrophoretic mobility

has no mass dependence.

In a desire to induce some mobility dependence on mass, DNA has been electrophoresed through gel matrices (2, 3, 4). The logic of this approach stems from the work of Ferguson (5) who found that in gels, the relative mobility of spherical proteins was inversely proportional to the logarithm of their molecular weights.

This behavior was attributed to the effects of sieving by the gel of different sized spheres. Since DNA in solution approximates a sphere (6), it was hoped that the electrophoretic mobility of DNA would also depend on the logarithm of the molecular weight in a gel system. The mobility of DNA in a 2.5% gel is inversely proportional to the log (molecular weight) for small DNA's. There is however, no dependence for DNA's of molecular weight greater than one million (2).

This lack of dependence can be understood if we examine the size of a large DNA in solution and compare this to the gel pore size. A DNA of molecular weight 10^8 would be expected to have a radius of gyration of about one micron (6). The pore size of a 2.5% gel has been experimentally found to be 0.035 microns (7). It is evident that a sphere of two microns diameter will not penetrate a gel with a pore size of

0.035 microns.

DNA molecules of this molecular weight though do enter and migrate in such gels easily. This behavior has prompted Aaij and Borst (4) to propose that such large molecules "crawl like snakes head on through the gels." Let us examine this model and then propose experiments to test it.

The main evidence for such a proposition is that the DNA free coil is much larger than the pore size and there is no dependence of mobility on molecular weight. The head on crawl model predicts that the DNA molecule should be stretched out, and oriented with the electric field. This prediction can be easily tested by electric dichroism.

In this experiment, in a gel, the DNA absorption at 260 nm is monitored in the presence and absence of a parallel electric field. It can be shown that for DNA, the maximum absorbance change for perfect alignment is 50% and in general for the DNA (8)

$$\Delta A_{260}/A_{260} = (3/4)(\langle \cos^2 \theta \rangle - (1/3))$$

where θ is the angle between the axis of the DNA helix and the electric field - optical axis. The derivation of this equation (for the equivalent flow dichroism experiment) is given by Callis and Davidson (8),

equations 13 through 18. In summary, the head on crawl model predicts the DNA molecule migrating in a gel should be stretched out, which is easily tested by electric dichroism. It should be noted that at the low electric fields used for electrophoresis, there would be no electric dichroism in the absence of the constraints imposed by the gel.

The head on crawl model also predicts that the molecule should remain stretched out for a long time after the field is removed. Lateral diffusion is prevented by the gel, only linear diffusion is allowed. The relaxation then should take a long time especially compared to the case of DNA in free solution (9), where the molecule can collapse volumetrically to its random coil configuration.

The extent of electric dichroism and the subsequent relaxation kinetics should provide adequate information to evaluate the proposed head on crawl model.

Bibliography

- 1) B. M. Olivera, P. Baine, N. Davidson, Biopolymers, 2, 245, 1964.
- 2) C. W. Dingman, M. P. Fisher, T. Kakefuda, Biochemistry, 11, 1242, 1972.
- 3) M. P. Fisher, C. W. Dingman, Biochemistry, 10 1895, 1971.
- 4) C. Aaij, P. Borst, Biochim. Biophys. Acta, 269, 192, 1972.
- 5) K. A. Ferguson, Metabolism, 13, 985, 1964.
- 6) P. J. Flory, "Principles of Polymer Chemistry", Cornell University Press, Ithica, New York, 1953.
- 7) G. W. Ackers, R. L. Steere, Biochim. Biophys. Acta, 59, 137, 1962.
- 8) P. K. Callis, N. Davidson, Biopolymers, 7, 335, 1969.
- 9) P. K. Callis, N. Davidson, Biopolymers, 8, 379, 1969.

Proposition 3

A Self Consistent, Realistic, Definition of
Resolution for Electron Microscopy

A definition of resolution is proposed. With regard to this definition, the effects of noise, contrast, vibration, and specimen drift are investigated. The resolution of the eye - microscope system and the photographic recording process are also discussed.

The resolving power of an electron microscope is an oft quoted value that intends to quantitate the smallest details observable using the instrument. Different techniques have been used to measure this value. Vacuum evaporated gold films are examined (on a photographic enlargement) at high magnification and the minimum spacings visible between gold clusters is taken as the resolution. Another technique is to examine a periodic structure such as a crystal, and try to observe the known spacing pattern. These techniques, as well as others, give different results and therefore make the term "resolution" rather meaningless.

For the present, resolution will be defined as the value of the uncertainty in position of an object

in object space. This uncertainty in position arises from both theoretical and practical considerations. Theoretically, the finite wavelength of the electron, the small angular aperture of the objective lens and various lens aberrations place a lower limit on the resolution obtainable. The specimen support film and specimen contrast also provide practical limits to the resolution.

In the light of the above definition of resolution, let us examine how to locate the edge of a thin film in the electron microscope. For the moment, let us ignore diffraction effects, the different index of refraction of the film, and let us assume the microscope has been properly focussed. If we measure the electron flux, I , at the image plane where the edge lies, we find

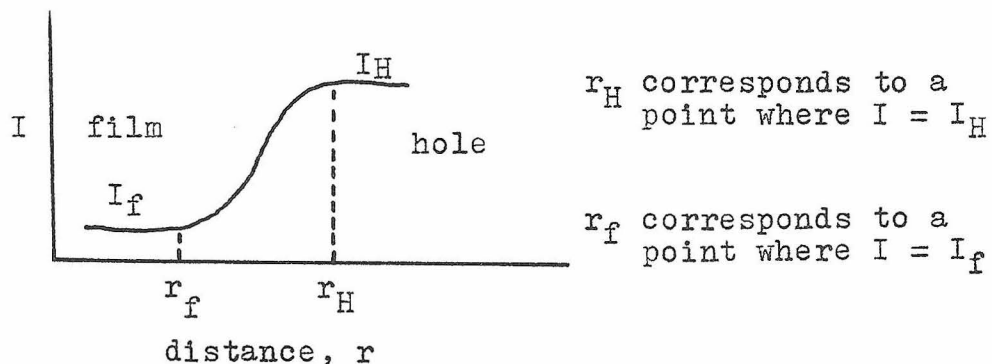


Figure 1. I versus r across the edge of semi-transparent film.

If on the image plane we measure a current flux, I_f , we know we are at a point on the image that corresponds to the film, measuring I_H , implies the hole. The film scatters some electrons into the objective aperture so at the image plane, the region corresponding to the film has a lower current flux (electrons $\text{sec}^{-1}\text{cm}^{-2}$) than the region corresponding to the hole. Since the information is contained in the current flux, this parameter rather than the darkening of a photographic plate, should be measured.

The probability of being in the hole region at a point on the image plane with current flux, I , is:

$$P(H) = \frac{I - I_f}{I_H - I_f} \quad (1)$$

The probability for being at a point corresponding to the film is:

$$P(f) = 1 - P(H) = \frac{I_H - I}{I_H - I_f} \quad (2)$$

The edge lies at a point where the film is on one side and the hole is on the other. We can locate the edge then only to the extent that we know the location of both the hole and the film. Since we need to know the location of both, the probability of finding the

edge between r_f and r_H is $P(f)_{\text{at } r_f} \times P(H)_{\text{at } r_H}$. We are

certain that the edge lies between r_f and r_H since

$$\begin{aligned} P(f)_{\text{at } r_f} &= P(H)_{\text{at } r_H} = 1 \quad \text{and} \\ P(f) \times P(H) &= 1 \end{aligned} \tag{3}$$

The resolution for this simple case is then the corresponding distance $r_H - r_f$ in object space. In a real case, it will be more practical to let $P(H) = 0.9$ etc. so that the probability of the edge being between r_f and r_H is 0.81. It is important to realize that no photographic or electronic means can improve this resolution. We are limited by our knowledge of the location of the film r_f , and the hole r_H . The resolution cannot be improved without knowing these locations more precisely.

In this simplistic approach, it is easy to write equations for $P(f)$ and $P(H)$. In an actual experiment, plots of I versus r across the edge of a cellulose nitrate film show scattering, interference, and phase effects (1, 2, the preparation of such films is described in ref. 3). The actual curve obtained, for a trace equivalent to that of figure 1 is shown in figure 2 and is from the work of Haine and Mulvey in 1954 (2).

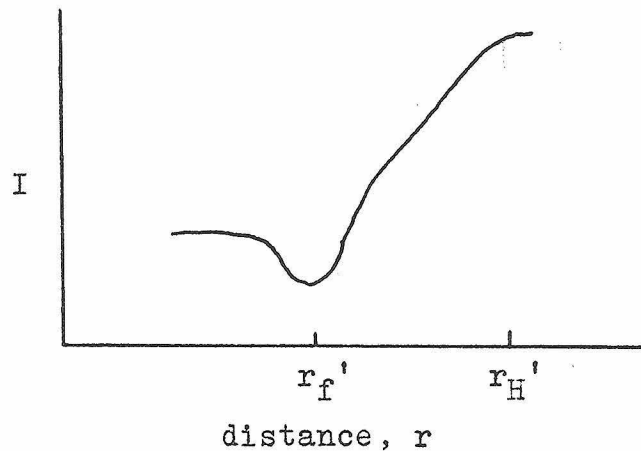


Figure 2. I versus r across the edge of a semi-transparent film. Experimental data from Haine and Mulvey. This figure actually represents the density on an in focus micrograph.

The shape of the curve differs from the ideal case because the semitransparent film has a different index of refraction than the hole, and some phase delay is introduced. It is however reasonable to assign r_f' and r_H' to the first minima and maxima respectively. It is proposed to use the distance $r_H' - r_f'$ in the object plane as a quantitative measure of resolution. It has the advantage of being independent of photographic enhancement techniques, it is sensitive to noise, contrast, focus, vibration, specimen drift, and can be relatively easily measured.

The usefulness of this definition of resolution is apparent when we examine how $r_H' - r_f'$ changes with the above perturbations. Contrast, I_H/I_f , and noise, ΔI_f , are related. As the contrast increases with

constant noise, the first minima and maxima become easier to identify (can be more accurately measured) and $r_H' - r_f'$ can be minimized. It must be remembered that r_f' is a point that is known (at least to a certain probability) to be on the film etc. . Increased noise requires increasing $r_H' - r_f'$ to insure knowing that r_f' and r_H' correspond to the film and hole regions respectively.

The effect of focus on $r_H' - r_f'$ was demonstrated experimentally by Hillier and Ramberg. They found a linear relationship between the square root of the out of focus distance, L , and the distance between the minima and maxima ($r_H' - r_f'$), (1).

$$(r_H' - r_f') = a (L)^{\frac{1}{2}} + b \quad (4)$$

In this equation, L is the distance between the object plane and the object, and b is the resolution at perfect focus.

Both vibration and drift increase $r_H' - r_f'$ by their respective magnitudes.

The resolution measured by this technique is objectively defined and is responsive in a reasonable manner to known perturbations. Since however, most electron microscopic images are recorded on film or examined on a fluorescent screen by means of the eye,

it is of interest to examine the resolution and noise of these systems.

In the eye - microscope system, the overall resolution will be that of the poorest member. There are four members to the group:

1. The specimen
2. The electron optical system
3. The fluorescent screen and binocular viewer
4. The eye

The dependence of resolution on 1 and 2 have been previously discussed. The fluorescent screen has a resolution of about 40 lines/mm, (3), and is usually viewed by means of a low power binocular microscope. The resolution of this combination is readily calculated. The resolving power of the fourth member of the group, the eye, is a more complicated function.

The response of the eye to the U. S. A. F. three bar target is presented in figure 3, (4). The target was examined with one eye and illuminated with green light having 6×10^{15} photons/ lumen sec. The figure indicates the locus of points where the three bars were just discernable as a function of brightness (apostilbs), period (α), and contrast.

The figure has several interesting features. The slope of the lines is about minus two. This implies

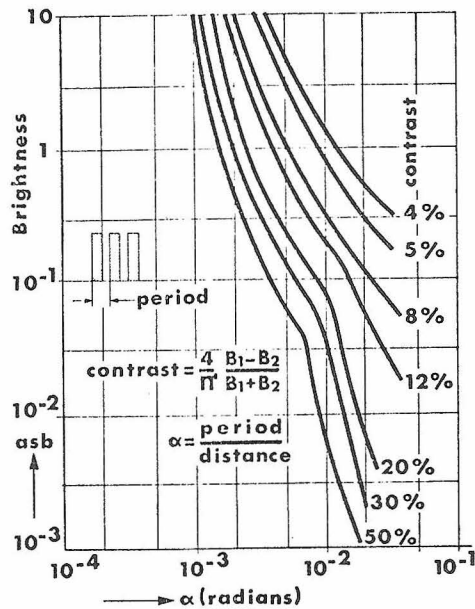


Figure 3. Response of the eye to the U. S. A. F. target.

that once the microscope is operating at crossover (maximum illumination), increasing the magnification will not help one resolve an object visually. This occurs because at fixed illumination,

$$\log(\text{brightness}) = -2\log(\alpha) \quad (5)$$

where (α) is proportional to the magnification.

The effect of contrast is also shown. The resolution of the eye increases (α becomes smaller) as the contrast increases. Since underfocussing the electron microscope is known to degrade the resolution,

but at the same time increase the contrast, we should examine this interplay in the light of overall resolution of the eye - microscope system.

Equation (4) shows how the resolution is degraded by defocus. The corresponding contrast enhancement may be either calculated (5, 6) or measured. Erickson and Klug (6) give 800 Å as the best value of underfocus, degrading the resolution of a Phillips EM 300 electron microscope to 20 Å.

Therefore I conclude that if the resolution is limited by the eye, increasing the contrast by underfocus will increase the overall resolution of the eye - microscope system. If sufficient brightness is available at high magnification, the overall resolution need be only limited by the specimen or electron optics.

Next, let us examine what happens when an electron image is recorded on film. This process clearly degrades the primary information, the electron current flux at each point in the image plane.

In this process, a layer of small, close packed grains of silver halide is exposed to the electron image. As electrons pass through the small grains, they occasionally initiate decomposition causing a part of that grain to be readily reduced to silver metal by a later chemical treatment. The darkening of the processed

plate is a function of the electron dose, but much noise is added to the signal by the process. The noise arises from many sources, some of them are:

1. Variation in grain size and therefore a variable target area for electrons.
2. The amount of reduced silver from a one electron "hit" is quite variable (7, 8).
3. A fine grained close packed monolayer of emulsion, yielding maximum resolution, gives only one developed grain per 12 electrons so that most of the information is just lost (7).

Although the photographic process is convenient, it certainly loses much of the information, and because it is a statistical process, it adds noise. Such a process then degrades the resolution. The most severe limitation is in the recording of the current flux. Scanning an evenly exposed and developed "high resolution" film with a 48 micron aperture yields a gaussian distribution of densities with a standard deviation of $1\frac{1}{2}\%$, (8). To lower this standard deviation, a larger aperture must be used.

I conclude then, that to record the current flux accurately (to a $1\frac{1}{2}\%$ standard deviation), the magnification must be great enough such that the inherent specimen - electron optical resolution is greater than 48 microns in the image (film) plane.

Bibliography

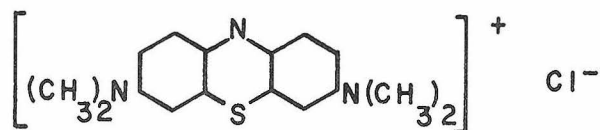
- 1) Hillier, Ramberg, J. Appl. Phys., 18, 48, 1947.
- 2) Haine, Mulvey, J. Sci. Instrum., 31, 326, 1954.
- 3) J. Reisner, "Scientific Instruments", 9, 1, Jan., R.C.A. publisher, 1964.
- 4) A. Nawijn, J. Cueleneare, "Performance of the Eye at Low Luminances", Proceedings of the Colloquium, Delft 1965, Excerpta Medica Foundation, Amsterdam 1966.
- 5) G. R. Grinton, J. M. Cowley, Optik, 34, 221, 1971.
- 6) H. P. Erikson, A. Klug, Berichte der Bunsen Gesellschaft, 74, 11, 1129, 1970.
- 7) L. Bachmann, M. M. Salpeter, Lab Invest., 14, 1041, 1965.
- 8) "Kodak Plates and Films for Science and Industry", Eastman Kodak Co., 1st. edition, 1967.

Proposition 4

The Binding Site for Methylene Blue
on Condensed κ Carrageenan

Methylene blue is a vital dye which exhibits an extrinsic Cotton effect upon binding to the condensed polysaccharide, κ carrageenan. The Cotton effect disappears when the condensed (gelled) polysaccharide is melted. An experiment is proposed to determine the binding site on the gelled polysaccharide.

Methylene blue (C.I. basic blue 9) is one of the most widely used biological stains (1). Its structure is

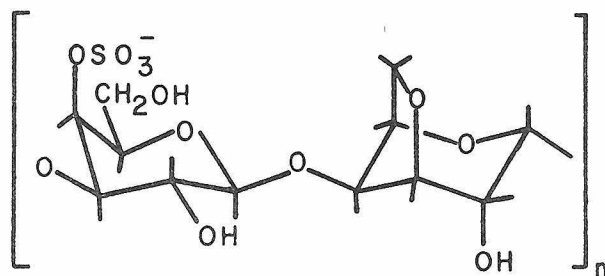


The positive charge explains the binding of this dye to acidic substances such as nuclei. This vital stain is also used for staining some bacteria (1), nerve tissue (1), and reportedly stains the golgi complex selectively (2).

The mode of binding to DNA (3) and to a negatively charged polysaccharide (4) (κ carrageenan) is more complicated than just ionic association as

the dye displays an extrinsic Cotton effect on binding. This behavior indicates that the dye binds in a unique manner, and allows further analysis of the binding. For DNA, flow dichroism studies indicate the dye binds by intercalation (3). Before proposing an experiment to determine the binding site for k carrageenan, we must examine the properties of this polysaccharide.

K carrageenan is a gel forming polysaccharide of the structure



It occurs naturally in marine algae and many types of animals (5). The following polysaccharides are structurally related to k carrageenan: hyaluronic acid, chondroitin, dermatan sulfate, keratan sulfate, agarose, porphyran, and furcellaran (5). Thus, binding studies of methylene blue to k carrageenan may also provide insight into the binding to, and structure of other polysaccharides.

The intent of the proposed experiment is to obtain flow orientable segments of k carrageenan and study the flow dichroism of methylene blue bound to those segments. This may be accomplished in the following manner.

K carrageenan can form a gel when the proper concentration of polysaccharide is cooled. It is postulated the structure of such a gel is a network of double helical regions joined by single strands of polysaccharide (4). The helicies extend until they encounter a "kink" in one of the polysaccharide chains. These kinks have been chemically identified (5, 6) and it is possible to cleave the k carrageenan chains at these "kink" residues (7).

K carrageenan cleaved in this fashion has a chain length of 30 to 40 disaccharide residues and does not form a gel (7). As a hot solution of this cleaved material is cooled in the presence of methylene blue, the dye exhibits circular dichroism as the normal gelling temperature is reached. Physical methods indicate a doubling of the k carrageenan molecular weight during this transition. X ray work on fibers of k carrageenan and computer model building indicate the structure is a double helix (8). It

has been proposed that the lack of gelling is due to the absence of single stranded polysaccharide chains tying the helical regions together (4). The double helical segments (8) of 30 to 60 disaccharide units (4) should have a length of 260 Å to 500 Å which allows them to be flow oriented (ref. 9, p. 444 describes the flow orientation of serum albumin with a length of 200 Å).

The transition moments for the various absorption bands in methylene blue need to be investigated. These data are not available at present, but are obtainable by quantum mechanical calculations or other experimental means.

The probability of absorption of light is proportional to $\cos^2 \theta$ where θ is the angle between the transition moment of methylene blue and the electric vector of the light. Let us consider three simple orthogonal orientations of the dye with respect to the helix (flow) axis, Z, and assume that one of the transition moments is in the plane of the molecule and parallel to the long axis (\parallel), and another is in the plane and perpendicular (\perp). These orientations are presented graphically in figure 1.

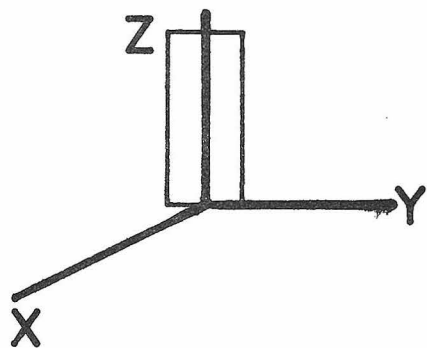
The flow orientation causes the Z axis to be fixed, but the molecule is free to rotate about the Z axis so no distinction is made between the X and Y axes.

Figure 1. Three orthogonal orientations for the binding of methylene blue to κ carrageenan. The location of two hypothetical transition moments are shown below.

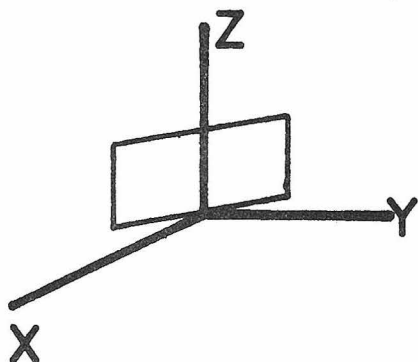
Plane of Dye

Binds || to Z

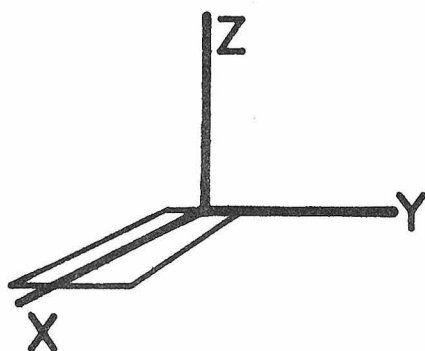
⊥ to X or Y



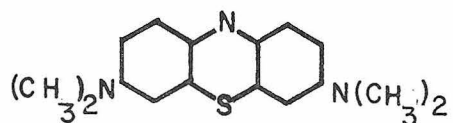
Same as above



Binds in X-Y Plane



Parallel
Transition



Perpendicular
Transition

FIGURE I

It is experimentally possible to orient the electric vector of the light parallel to the Z or X axis. Let us examine how models I, II, and III would respond to polarized light. In the experiment, the absorbance with no flow is subtracted from the absorbance with flow orientation. A plus sign (+) indicates the result is positive, a negative (-) indicates either no change or less expected absorbance during flow orientation.

Table 1

transition moment	light polarized to Z axis		light polarized to X axis	
		⊥		⊥
Model				
I	+	-	-	+
II	-	+	+	-
III	-	-	+	+

It is also possible by graphical means (11) to determine the angle between the transition moment and the flow axis.

This experiment should allow the unambiguous assesment of the bonding site of methylene blue to k carrageenan.

Bibliography

- 1) R. D. Lillie "H. J. Conn's Biological Stains"
8th edition, William and Wilkins Co., Baltimore
1969.
- 2) A. C. Giese, "Cell Physiology", 3rd edition, W. B.
Saunders Co., Philadelphia, 1968.
- 3) F. E. Hahn, A. K. Kreg, Antimicrobial Agents and
Chemotherapy, p. 15, 1969.
- 4) I. C. M. Dea, A. A. McKinnon, D. A. Rees, J. Mol.
Biol., 68, 153, 1972.
- 5) D. A. Rees, I. W. Steele, F. B. Williamson, J.
Polymer Sci., 28, 261, 1969.
- 6) N. S. Anderson, T. C. S. Dolan, D. A. Rees, J. Chem.
Soc., C, 596, 1968.
- 7) A. A. McKinnon, D. A. Rees, F. B. Williamson,
Chem. Comm., 701, 1969.
- 8) N. S. Anderson, J. W. Cambell, M. M. Harding,
D. A. Rees, J. W. B. Samuel, J. Mol. Biol., 45,
85, 1969.
- 9) C. Tanford, "Physical Chemistry of Macromolecules",
Wiley, New York, 1961.
- 10) L. S. Lerman, Proc. Nat. Acad. Sci., 49, 94, 1963.
- 11) A. Wada, Biopolymers, 2, 361, 1964.

Proposition 5

On the Possibility of Heavy Atom Contrast
in the Scanning Electron Microscope

The backscattering coefficient for 30 KV electrons differs between light and heavy elements by a factor of 10. The backscattering coefficient for mixtures of light and heavy elements is formulated and the possibility of using "heavy atom stains" is discussed.

In conventional scanning electron microscopy, the secondary electron ($E < 50V$) current or the reflected electron ($E > 100V$) current is used for contrast. Both signals yield topological information about the sample as the currents are in general a function of the angle between the scanning electron beam and the specimen. The yield of secondary electrons is not a function of composition (1), while the fraction of backscattered electrons is (2). At 30 KV, the fraction of reflected electrons, η , is about 0.06 for carbon, 0.53 for uranium, 0.42 for silver, and 0.319 for copper (2). Since the yield is so different, it might be possible to use the effect to locate concentrations of high atomic number material in the presence of low atomic number background.

It is desired to formulate an equation which will predict the backscattering as a function of the uranium concentration in a background of carbon. Since the penetration depth of an electron is only a function of the mass traversed, let

$$\eta' = 0.06 X_b + 0.53 X_u \quad (1)$$

where X_b and X_u are the weight fractions of biological (carbon) material and uranium respectively. η' is the total expected backscatter coefficient.

If an equal mass of uranium binds, the expected backscattering coefficient is 0.3, a five fold increase over the carbon background. An equal mass of uranium of atomic weight 238 corresponds to one uranium atom to about 20 carbon atoms.

Let us now examine the question of resolution. When a high energy (30 KV) electron enters a specimen, it suffers many collisions. A small beam of several hundred angstroms diameter would perhaps spread 3 or 4 microns laterally before giving up most of its energy (3, 4, 5). If the electrons were reflected from all of this area, the resolution would be reduced to 6 or 8 microns. Although it is not easy to calculate the lateral diffusion versus depth relationship, the fraction of electrons transmitted through films of

varying thickness, is known. A film thickness that transmits most of the electrons cannot have much lateral electron movement within it.

The fraction of electrons of energy E_0 (in KV) that penetrated to a depth Z is given by

$$I(Z)/I(0) = \exp(-Z/Z_n)^p \quad (2)$$

where $p \cong 2$ for light elements (4, 5) and Z_n is the depth at which $1/e$ of the electrons are still transmitted.

$$Z_n = C E_0^n \text{ (ref. 5)} \quad (3)$$

where $C = 0.0034$, E_0 is in KV, and $n = 1.65$ for light elements and Z_n is in units of mg/cm^2 (the data are actually for aluminum). For the above example, $Z_n = 0.93 \text{ mg}/\text{cm}^2$.

It is proposed to stain chromosomes with a heavy metal and use this technique to map the location of that metal by reflected electron current measurements.

The dimensions and density of human chromosomes are given by DuPraw (6). The diameter of the chromosome arms is $\frac{1}{2} \mu$ and the density (dry) is $1.31 \text{ g}/\text{cm}^3$ and they are composed on the average of 15% DNA. Most 30 KV electrons are transmitted through a chromosome arm as:

$$Z = (1310 \text{ mg}/\text{cm}^3)(\frac{1}{2} \times 10^{-4} \text{ cm}) \quad (4)$$

and

$$I(Z)/I(o) = \exp(-.07/.932)^2 = 99.5\% \quad (5)$$

This result implies that there is little lateral spreading of the beam during passage through a chromosome. Even with the density doubled by the addition of uranium, $I(Z)/I(o)$ is still about unity. Thus the resolution inherent in the beam diameter is not appreciably degraded.

If one uranium were attached to one DNA phosphate, the contrast change $(\frac{\Delta\eta'}{\eta'})$ can be calculated.

$$X_b = 330/568 = 0.58 ; \quad X_u = 0.42 \quad (6)$$

$$\eta' = .035 + .222 = .257 \quad (7)$$

$$\Delta\eta'/\eta' = 4.3 \quad (8)$$

If chromosomes have any significant variation of DNA composition along their length, it should be possible to detect this by the backscattering contrast. It might also be possible to simultaneously divide some of the secondary electron signal into the reflected electron signal in order to remove the topological signal from the compositional signal.

The sample of course should have minimum topological variation and should be mounted on a thin film with an electron trap behind to remove the main beam.

Bibliography

- 1) K. G. McKay, Advances in Electronics, 1, 65, 1948.
- 2) H. E. Bishop, Ph D Dissertation, Cambridge, 1966.
or
P. R. Thornton, "Scanning Electron Microscopy",
Chapman and Hall Ltd. London, 1968.
- 3) A. Ya Vyatshin, A. F. Makhov, Soviet Physics -
Tech. Physics., 3, 690, 1958.
- 4) A Ya Vyatshin, A. F. Makhov, Soviet Physics
Solid State, 2, 810, 1960.
- 5) A. F. Makhov, ibid, 2, 1934, 1942, 1945, 1960.
- 6) E. J. DuPraw, "DNA and Chromosomes", Holt, Rinehart;
and Winston, Inc., New York, 1970.